

# Acceleration of expensive computations in Bayesian statistics using vector operations

David J. Warne<sup>\*†</sup>, Scott A. Sisson<sup>‡</sup> and Christopher Drovandi<sup>†</sup>

July 15, 2019

## Abstract

Many applications in Bayesian statistics are extremely computationally intensive. However, they are also often inherently parallel, making them prime targets for modern massively parallel central processing unit (CPU) architectures. While the use of multi-core and distributed computing is widely applied in the Bayesian community, very little attention has been given to fine-grain parallelisation using single instruction multiple data (SIMD) operations that are available on most modern commodity CPUs. Rather, most fine-grain tuning in the literature has centred around general purpose graphics processing units (GPGPUs). Since the effective utilisation of GPGPUs typically requires specialised programming languages, such technologies are not ideal for the wider Bayesian community. In this work, we practically demonstrate, using standard programming libraries, the utility of the SIMD approach for several topical Bayesian applications. In particular, we consider sampling of the prior predictive distribution for approximate Bayesian computation (ABC), the computation of Bayesian  $p$ -values for testing prior weak informativeness, and inference on a computationally challenging econometrics model. Through minor code alterations, we show that SIMD operations can improve the floating point arithmetic performance resulting in up to  $6\times$  improvement in the overall serial algorithm performance. Furthermore 4-way parallel versions can lead to almost  $19\times$  improvement over a naïve serial implementation. We illustrate the potential of SIMD operations for accelerating Bayesian computations and provide the reader with essential implementation techniques required to exploit modern massively parallel processing environments using standard software development tools.

*Keywords:* vectorisation; single instruction multiple data; advanced vector extensions; approximate Bayesian computation; weakly informative priors; parameter inference; sequential Monte Carlo.

---

<sup>\*</sup>Corresponding author: david.warne@qut.edu.au

<sup>†</sup>School of Mathematical Sciences, Queensland University of Technology, Brisbane, Australia

<sup>‡</sup>School of Mathematics and Statistics, University of New South Wales, Sydney, Australia

# 1 Introduction

The study of the posterior distribution is essential in applied Bayesian statistics. However, most practical applications are computationally challenging since the posterior probability density function (PDF) is only known up to a normalising constant. That is, given data,  $\mathcal{D}_{\text{obs}}$ , a theoretical stochastic model with parameter vector,  $\boldsymbol{\theta}$ , from some parameter space,  $\Theta$ , a prior PDF,  $\pi(\boldsymbol{\theta})$ , and likelihood function,  $\mathcal{L}(\boldsymbol{\theta}; \mathcal{D}_{\text{obs}})$ , the posterior PDF is

$$\pi(\boldsymbol{\theta} \mid \mathcal{D}_{\text{obs}}) = \frac{\mathcal{L}(\boldsymbol{\theta}; \mathcal{D}_{\text{obs}})\pi(\boldsymbol{\theta})}{\pi(\mathcal{D}_{\text{obs}})}, \quad (1)$$

where the evidence,  $\pi(\mathcal{D}_{\text{obs}})$ , is typically analytically intractable. Therefore, advanced Monte Carlo schemes are often required. The difficulty is compounded for applications with computationally expensive likelihoods or intractable likelihoods, which are increasingly commonplace (Sisson et al., 2018). Of course, sampling challenging posterior distributions is not the only computationally expensive problem in Bayesian statistics. For example, in some analyses that require some level of objectivity, it may be important for priors to be weakly informative, and selected from a family of priors  $\pi(\boldsymbol{\theta} \mid \boldsymbol{\lambda})$  with hyperparameter,  $\boldsymbol{\lambda}$  (Evans and Jang, 2011; Gelman, 2006). In this case prior-predictive  $p$ -values must be estimated for a large set of hyperparameter candidates, this requires the evidence density to be estimated, a computationally intensive task in itself, over samples from the prior predictive distribution (Nott et al., 2018).

While computational methods in Bayesian statistics continue to improve and evolve (Green et al., 2015), the computational performance of modern computer hardware is also increasing. Most computer processor improvements over the last decade are the result of increased capacity of parallel processing. Consideration of the implementation details for Monte Carlo algorithms is therefore essential if one is to fully exploit modern computational resources. The optimisation of codes for efficient use of hardware acceleration has become a standard technique to improve the performance of typical *high performance computing* (HPC) workloads.

Many Monte Carlo schemes lend themselves to parallel computing architectures. For example, likelihood-free methods, such as approximate Bayesian computation (ABC; Sisson et al., 2018) typically require generating a large number of independent simulations from the prior predictive distribution  $\pi(\mathcal{D}_{\text{obs}})$ . However, while direct Monte Carlo schemes may trivially be executed in parallel, other more sophisticated samplers, such as Markov chain Monte Carlo (MCMC) (e.g. Green et al., 2015; Marjoram et al., 2003), sequential Monte Carlo (SMC) (e.g. Del Moral et al., 2006; Sisson et al., 2007) and multilevel Monte Carlo (MLMC) (e.g. Beskos et al., 2017; Dodwell et al., 2015; Jasra et al., 2019; Warne et al., 2018) require more effort to efficiently parallelise (Mahani and Sharabiani, 2015; Murray et al., 2016) since there are synchronisation and communication requirements. In many cases, these overheads can inhibit the scalability of these algorithms across many central processing unit (CPU) cores.

General purpose graphics processing units (GPGPUs) have been demonstrated to be highly effective at accelerating advanced Monte Carlo schemes (Klingbeil et al., 2011; Lee et al.,

2010). GPGPUs make heavy use of *single instruction multiple data* (SIMD) operations (van der Pas et al., 2017), that is, a numerical operation that operates on a vector of data in an element-wise fashion. Such SIMD operations are also widely available in modern CPUs that now contain multiple vector processing units (VPUs). By exploiting the VPUs, CPU-based implementations can achieve performance boosts comparable with GPGPU implementations (Hurn et al., 2016; Lee et al., 2010; Mudalige et al., 2016). A practical understanding of how CPU vector operations function and how to access them in software is, therefore, highly relevant to applied Bayesian analysis. In this article, we focus on the code structures and algorithmic techniques that applied computational statisticians may utilise to take advantage of VPU technology that is available in the majority of commodity CPUs today. We also provide example code written in the C programming language as supplementary material<sup>1</sup>.

## 1.1 Parallel computing paradigms

For more than a decade, the fundamental speed of CPUs, in terms of clock frequency, has not changed significantly (Ross, 2008). Modern CPUs are typically clocked between 2 GHz and 4 GHz. Therefore, to increase the computational throughput, CPU architectures are now designed to perform multiple tasks in parallel. For computationally intensive tasks, such as those frequently encountered in Bayesian statistics, understanding how to exploit parallel computing architectures is essential.

There are several paradigms of parallelism, all of which may be relevant to the same computational task. The most fundamental paradigms are *distributed computing*, *multithreading*, *vectorisation*, and *pipelining* (Trobec et al., 2018; van der Pas et al., 2017). Though the combination of multithreading and vectorisation is the focus of this work, we briefly introduce all these paradigms for context.

*Distributed computing*: Computational tasks are shared across multiple computers, each with their own CPU and memory, that are connected via a high-speed network. This form of parallelism is the basis of HPC and high throughput computing (HTC).

*Multithreading*: Programs are divided into several processing streams, called threads, which may be executed independently. While multithreading is an important software design concept even for single core CPUs, modern multicore CPUs allow threads to truly execute concurrently. Since threads are part of the same program, they share the same memory and variables.

*Vectorisation*: In many modern CPUs, each core may perform one or more vector instructions using the VPU. These allow a single operation to be applied to multiple input operands in the same clock cycle.

*Pipelining*: Many CPU instructions involve multiple stages and take multiple clock cycles to complete. Often, it is possible for processing of the next instruction to commence before the current one is complete. This is implemented in the CPU hardware and occurs auto-

---

<sup>1</sup>Example code is available from GitHub: <https://github.com/davidwarne/Bayesian.SIMD.examples>

matically. However, it should be noted that some programming constructs may negatively affect this instruction pipeline: for example, a conditional statement. Some specialised devices, such as *field programmable gate arrays* (FPGAs) can also implement algorithm specific pipelining architectures.

Each of these parallel computing paradigms have a granularity, which refers to the communication to computation ratio of the parallel workload it supports. In this context, we refer to distributed computing and multithreading as coarse-grained, whereas vectorisation and pipelining are considered fine-grained.

The technology to achieve fine-grain parallelism has typically been accelerator co-processors. That is, specialised processors, typically packaged on an expansion card, that the CPU offloads fine-grain parallel workloads to. Unsurprisingly, most exemplars of fine-grain parallelism in the computational statistics literature is based on accelerators, such as GPGPUs (Lee et al., 2010; Terenin et al., 2018), Intel Xeon Phi (Hurn et al., 2016; Mahani and Sharabiani, 2015), and FPGAs (Fernandes et al., 2016; Zierke and Bakos, 2010).

The usage of accelerators is not practical for all practitioners of computational Bayesian statistics. As a result, we will not discuss them in any detail. Instead we highlight that the parallelisation strategies required to get the most out of these accelerators are also key to getting the most out of standard CPU hardware. In particular, the effective utilisation of vectorisation can boost the performance of CPU-based software.

## 1.2 Contribution

The aim of this article is to present the utility of the modern CPU-based SIMD operations to accelerate computational Bayesian inference through practical demonstration. We present several topical case studies involving compute intensive tasks. Specifically, we investigate: (i) sampling of the prior predictive distributions for approximate Bayesian computation (Sisson et al., 2018; Sunnåker et al., 2013); (ii) computation of Bayesian  $p$ -values for prior weak informativity tests (Evans and Jang, 2011; Gelman, 2006; Nott et al., 2018); (iii) and parameter inference for a computationally intensive econometrics model (Bekaert et al., 2015; South et al., 2019; Li et al., 2019). As we progress through each case study, we highlight the key algorithmic features that are appropriate for fine-grain and coarse-grain parallelism and demonstrate modifications to provide guidance to the practitioner. Given the scarcity of exemplars in statistics using SIMD operations, we believe a clear demonstration of additional performance benefits is a significant contribution to the computational statistics community.

We specifically focus on the additional performance boost available through SIMD operations on modern commodity CPU hardware. Therefore, we do not provide comparisons with dedicated accelerator coprocessors, such as GPGPU, Intel Xeon Phi, and FPGA accelerators as this has been covered in some detail in the HPC literature (Dongarra et al., 2014; Halyo et al., 2014; Teodoro et al., 2014; Wang et al., 2014; Warne et al., 2014; Zohouri et al., 2016). However, it should be noted that our methods are directly applicable to these technologies and furthermore our code will run on the in-socket variants of the Intel Xeon Phi

without any modifications.

All of our code is written in the C programming language. We utilise the OpenMP standard (version 4.5) to implement multithreading and vectorisation. Random number generators (RNGs) are provided by the Intel Math Kernel Library (version 2018). Compiled binary applications are built using the Intel compiler, `icc`. All case study codes, compiler options, and inputs are provided within the supplementary material. While we provide stand-alone C implementations, it is important to note that our algorithm design and implementation guidelines are also completely relevant to the MATLAB C MEX<sup>2</sup> and Rcpp (Eddelbuettel and Francois, 2011) interfaces.

The remainder of this article is organised as follows: In Section 2, we introduce the fundamental programming constructs for exploiting SIMD operations. Where appropriate, example code is provided. In Sections 3, 4, and 5, we present our case studies on prior predictive sampling for ABC, weak informativity tests, and econometrics parameter inference, respectively. In each case study, we present briefly any essential background theory, highlight the opportunities for parallelisation and vectorisation, demonstrate the steps taken to implement and optimise the computational problem. Performance improvement results are presented for two families of CPU architecture, namely, Haswell and Skylake. Section 6 provides a discussion of the results and the strengths and weaknesses of SIMD operations from the perspective of applied Bayesian statisticians.

## 2 A guide to vectorisation

In this section, we provide some necessary CPU computing concepts that we draw upon in our case studies. We avoid discussing low-level technological details in favour of providing simple programming tools that may be directly applied to other Bayesian applications.

### 2.1 Parallel random numbers

Regardless of the computing architecture, a particularly important topic to consider when applying parallel computing techniques to statistical applications is parallel random number generation. Dealing with this poorly can lead to results that are statistically biased. We do not focus on specifics of this problem, as the topic is well documented (Bradley et al., 2011; Lee et al., 2010). However, we simply state the three main approaches:

1. Generate all required randomness serially on the host processor and distribute among parallel processes;
2. Use a random number generator that can be split into independent sub-streams, for example a generator that supports *Skip Ahead* or *Leapfrog* methods;

---

<sup>2</sup>See MATLAB documentation pages, [https://www.mathworks.com/help/matlab/call-mex-files-1.html?s\\_tid=CRU](https://www.mathworks.com/help/matlab/call-mex-files-1.html?s_tid=CRU)

- Use a sequence of random number generators that are statistically independent for the same seed value.

While it is common to simply use different seed values for the same RNG, caution is advised as this may not always be statistically valid. For example, it has been shown that sequences of Linear Congruential Generators can become correlated if a linear sequence of seeds is used (Davies and Brooks, 2007).

In all of our work, we utilise the `VSL_BRNG_MT2203` generator family which is available in Intel Math Kernel Library (MKL). The `VSL_BRNG_MT2203` generator family provides 6,024 statistically independent Mersenne Twister (Matsumoto and Nishimura, 1998; Mikhailov, 2001) generators.

## 2.2 SIMD operations

The traditional view of a CPU core is a purely sequential processor, performing exactly one operation each clock cycle. An operation might involve reading/writing data or performing an arithmetic calculation. With this assumption, the loop in Figure 1(a) will require four floating point addition operations within the loop body. See Tian et al. (2013) for a more technical discussion on SIMD operations.

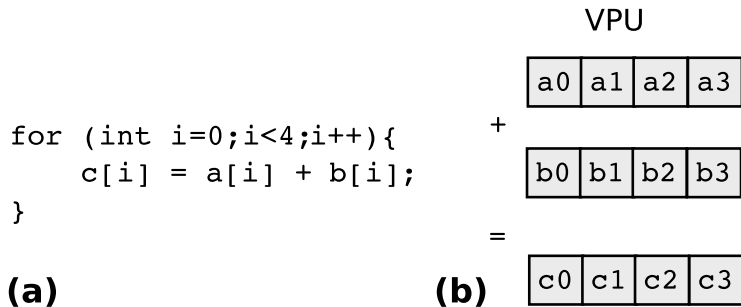


Figure 1: VPUs execute SIMD operations. The body of the `for` loop in (a) can be implemented with four scalar additions, or alternatively as one vector addition as shown in (b). If the elements in arrays `a`, `b`, and `c` are single precision floating point numbers, then 128-bit vector registers are required. Otherwise, for double precision floating point numbers, then 256-bit vector registers are required.

While modern CPU cores are still sequential<sup>3</sup>, arithmetic operations may be scalar or vector. While Figure 1(a) would take four *scalar* additions, only a single *vector* addition may be required, representing a speedup factor of four.

Most modern CPUs have VPUs. The inputs to these units are wider than the scalar arithmetic logic units (ALUs). For example, the VPU may accept 256-bit vector inputs, this could store eight single precision (32-bit) floating point numbers or four double precision

<sup>3</sup>Although, they do not necessarily execute operations in the order defined by the users code. CPUs re-order operations as needed to optimise pipelining. This is called out-of-order execution and is a feature that is not readily available on accelerator architectures.

(64-bit) floating point numbers. The VPU performs element-wise arithmetic on the input vectors as shown in Figure 1(b).

Speedups attained through the usage of vector operations are in addition to performance gain through multithreading. Using four threads and 512-bit vectors could perform up to  $4 \times (512/64) = 32$  times as many double precision operations per second than sequential and scalar operations.

## 2.3 Vectorisation and multithreading with OpenMP

Just as with multithreaded parallelism, there are many ways to access the VPUs in algorithm implementations. In this work, we focus on usage of `OpenMP`, an open standard for automated parallel computing. `OpenMP` allows developers to write standard C/C++ or FORTRAN code, and supports parallel computing through the insertion of *directives* (van der Pas et al., 2017). That is, statements that hint to the compiler, that a section of code may benefit from threading or vectorisation. All of the lower-level, technical details are dealt with by the compiler.

```
#pragma omp simd
for (int j=0;j<N;j++){
    c[j] += a[j]*b[j];
}
```

Figure 2: Example loop vectorisation, which the compiler will attempt to transform into vector operations.

For example, placing the directive `#pragma omp simd` before a loop, as in Figure 2, tells the compiler to attempt to re-formulate the loop using vector operations. Similarly, the directive `#pragma omp parallel` tells the compiler to create a worker pool of threads for within the next code block. From within a parallel block, using the directive `#pragma omp for` before a loop will cause the iterations to be distributed across the threads in this worker pool. For example, Figure 3(a) shows the same loop as in Figure 2, but here the parallelisation comes from using multiple cores. An equivalent shorthand directive is shown in Figure 3(b).

Figure 2 and 3 are demonstrations of the `OpenMP` directives only. In practice, real codes will have multiple nested loops, and determining when to use `simd` (Figure 2), `parallel` and `for` (Figure 3(a)), and `parallel for` (Figure 3(b)) is key to our case studies. The following guidelines useful to keep in mind:

1. Use `simd` (Figure 2) when each loop iteration is completely independent with no branch conditions and data arrays are small. The loop body must also be simple, involving only arithmetic and standard mathematical functions (e.g. `sin`, `cos`, `exp` or `pow`).



L1 cache, then L2 is checked and so on. Finally, RAM is accessed if the data is not in any level of cache. Every failed cache access is called a cache miss.

The goal is to access data arrays in such a way that the number of cache misses is minimised. Key guidelines are:

- Access memory in a regular pattern. For example, access `a[i]`, then `a[i+n]`, then `a[i+2*n]` and so on. Ideally, `n` (called the stride) is small (and `n = 1` is preferred)<sup>5</sup>.
- Aim to reuse data soon after it was last accessed. If a partial calculation is pushed out of cache and into RAM, then it might be faster to re-compute every time rather than access RAM again.

Another important memory consideration for vector operations is memory alignment. Memory is partitioned into blocks called cache lines. For the CPUs we consider, these are 64 bytes in length. When the CPU loads data at a particular memory address, the entire cache line is loaded. Therefore, when doing vector operations, it is important that the first byte of a data array is aligned with the 64-byte cache line boundaries, otherwise some vectors cross over cache line boundaries. Trying to perform vector operations on unaligned data incurs a performance penalty. In practice this means:

- For dynamic memory, default `malloc` or `new` commands cannot be used (they often default to a 8byte or 16byte boundary. Instead, use either Intel's `_mm_malloc` or GNU's `memalign`).
- For static arrays append `__declspec(align(64))` to the array declaration. For example, `__declspec(align(64)) double A[100]` is a 64-byte aligned array.

This is a somewhat minor code alteration. It is important to note that, with modern processors, vector operations can still be applied to unaligned data, but every time a vector crosses a cache line boundary there is an extra read operation penalty.

Efficient use of cache and memory access patterns is a large topic, and we only aim to highlight common features that we will utilise in our case studies. See for example, Crago et al. (2018); Edwards et al. (2014); Eichenberger et al. (2004); Geng et al. (2018); Pennycook et al. (2013) and the monologue by Levesque and Wagenbreth (2010) for further discussion on memory access considerations.

## 2.5 Performance analysis

Many optimisation decisions and hardware comparison benchmarks are made without proper analysis of the original unoptimised implementation of an algorithm (Hurn et al.,

---

<sup>5</sup>Access matrices according to the matrix storage format. In C/C++, the row-major format is used, that is for a matrix `double A[N][M]` matrix element `A[i][j]` is equivalent to the linear index `A[i*M + j]`. So access should proceed row-by-row

2016; Lee et al., 2010). This can be costly in terms of development time or new hardware purchases. Here, we provide some important guidelines that should assist in assessing how efficient a statistical application is, before code optimisation or acceleration is considered.

1. Use a profiler and static code analysis software. A profiler will monitor the execution of running software and report time spent in each line of code. Also information like memory latency, cache miss frequency and peak floating point performance can be reported. Static code analysers do not run the code, but look for particular patterns and provide recommendations. In this article we utilise the Intel VTune Amplifier and Intel Advisor tools.
2. Estimate the theoretical peak performance. How many floating point operations does the code, on average, perform? What is the theoretical peak of the available CPU?
3. The maximum performance improvement from multithreading and vectorisation is limited by the operations that cannot be parallelised or vectorised. Most algorithms require some sequential only operations, and not all floating point calculations can be efficiently mapped to vector operations. Amdahl’s law (Amdahl, 1967) provides a useful expression to evaluate the speedup opportunity for a given program with profile data. That is, the speedup factor,  $s$ , is bounded by

$$s \leq \frac{C_S + C_P}{C_S + C_P/P}, \quad (2)$$

where  $C_P$  is the sequential runtime of code that can be parallelised/vectorised,  $C_S$  is the runtime of code that must remain sequential, and  $P$  is the number of cores/vector length. Hence, as  $P \rightarrow \infty$  we have  $s \leq (C_S + C_P)/C_S$  as a measure of the extent to which the algorithm may ideally utilise parallel architectures.

## 2.6 Summary

In this section, we have provided generic guidelines in the areas of parallel RNGs, vectorisation, multithreading, memory usage and code analysis. Other than parallel RNG, most of these guideline are not specific to Bayesian statistics, however, they are practical and easy to implement in any statistical codes that are based on fundamental languages like C/C++ and FORTRAN (we leave until the discussion in Section 6 to highlight issues with higher-level languages in these aspects). In the remainder of this article, we demonstrate these guidelines practically through topical Bayesian applications.

## 3 Prior predictive sampling

Approximate Bayesian computation (ABC) techniques are one class of likelihood-free methods that provide a powerful framework for the approximate sampling of posterior distributions when the likelihood function is computationally intractable (Sisson et al., 2018;

Sunnåker et al., 2013). The most accessible algorithm for applied practitioners is the *ABC rejection sampler* (Tavaré et al., 1997), that generates artificial data from the prior predictive distribution,

$$\pi(\mathcal{D}) = \int_{\Theta} \mathcal{L}(\boldsymbol{\theta}; \mathcal{D}) \pi(\boldsymbol{\theta}) d\boldsymbol{\theta}, \quad (3)$$

and accepts a small proportion of them as samples from an approximation to the posterior  $\pi(\boldsymbol{\theta} | \mathcal{D}_{\text{obs}})$  based on a discrepancy measure against the observational data.

Given observed data,  $\mathcal{D}_{\text{obs}}$ , the parameter prior distribution,  $\pi(\boldsymbol{\theta})$ , a discrepancy function,  $\rho$ , and a vector of sufficient (or informative) summary statistics  $S(\mathcal{D}_{\text{obs}})$ , then a simple version of the ABC rejection method generates posterior samples as given in Algorithm 1.

---

**Algorithm 1** ABC rejection sampling

---

- 1: **repeat**
  - 2:   Generate prior sample  $\boldsymbol{\theta}^* \sim \pi(\boldsymbol{\theta})$ ;
  - 3:   Use stochastic simulation to generate prior predictive data  $\mathcal{D}^* \sim \mathcal{L}(\boldsymbol{\theta}^*; \mathcal{D})$ ;
  - 4: **until**  $\rho(S(\mathcal{D}_{\text{obs}}), S(\mathcal{D}^*)) \leq \epsilon$ ;
  - 5: Accept  $\boldsymbol{\theta}^*$  as an approximate posterior sample;
- 

In practice, ABC rejection sampling is rarely implemented in this manner. A more practical and effective means for performing ABC rejection, especially in parallel, is to generate a fixed number,  $N$ , of prior predictive joint samples,  $(\boldsymbol{\theta}^*, \mathcal{D}^*)$  (Algorithm 1 is serial, and generates a random number of model simulations to produce a single ABC sample). The acceptance threshold,  $\epsilon$ , is then selected *a posteriori* based on the empirical distribution of the discrepancy metric,  $\rho$ , for these samples. See Fan and Sisson (2018) and Warne et al. (2019) for detailed reviews of ABC Monte Carlo algorithms.

ABC methods are routinely used in the study of complex stochastic models (Beaumont et al., 2002; Browning et al., 2018; Drovandi and Pettitt, 2011; Johnston et al., 2014; Ross et al., 2017; Tanaka et al., 2006; Vo et al., 2015; Rodrigues et al., 2019). However, Monte Carlo estimators based on ABC converge slowly in *mean-square* compared with exact Monte Carlo sampling algorithms (Barber et al., 2015; Fearnhead and Prangle, 2012). The ABC rejection method naturally lends itself to multithreading, and distributed parallelism. However, the opportunities for SIMD level parallelism depend on the model. In this section, we demonstrate these opportunities through two illustrative inference problems with intractable likelihoods.

### 3.1 Model examples

We provide two example models, selected to demonstrate the advantages and limitations of SIMD parallelism compared with thread parallelism under ABC rejection sampling. Both models are Markov processes, however, one is discrete and the other is continuous in time. The continuity of time, for the task of generating a large number of prior predictive samples, turns out to be the main factor affecting the efficacy of SIMD operations.

### 3.1.1 Genetic toggle switch

We use the genetic toggle switch model of Bonassi et al. (2011), also considered by Vo et al. (2019). We let  $u_i(t)$  and  $v_i(t)$  represent the expression levels of genes  $u$  and  $v$  at time  $t$  for cells  $i = 1, 2, \dots, C$ . The state of each cell evolves according to two coupled *stochastic differential equations* (SDEs), which are discretised according to the *Euler-Maruyama* scheme with timestep,  $\Delta t$ , so that

$$\begin{aligned} u_i(t+h) &= u_i(t) + \Delta t \frac{\alpha_u}{1 + v_i(t)^{\beta_u}} - \Delta t(1 + 0.03u_i(t)) + 0.5\xi_{i,u}(t), \\ v_i(t+h) &= v_i(t) + \Delta t \frac{\alpha_v}{1 + u_i(t)^{\beta_v}} - \Delta t(1 + 0.03v_i(t)) + 0.5\xi_{i,v}(t), \end{aligned} \quad (4)$$

where the parameters  $\alpha_u$ ,  $\beta_u$ ,  $\alpha_v$  and  $\beta_v$  define repressive responses and  $\xi_{i,u}(t)$  and  $\xi_{i,v}(t)$  are independent normal random variables with variance  $\Delta t$ .

For inference, only gene  $u$  is measured with error for each cell at a fixed time  $T$  according to

$$y_i = u_i(T) + \mu + \mu\sigma \frac{\eta_i}{u_i(T)^\gamma}, \quad i = 1, 2, \dots, C, \quad (5)$$

where  $\mu$ ,  $\sigma$  and  $\gamma$  control the error rate and the  $\eta_i$  are standard normal random variables. A set of the measurements across all cells,  $\{y_i\}_{i=1}^C$ , constitutes a dataset. We consider sampling of the prior predictive distribution for the purposes of estimation of the parameters  $\theta = (\alpha_u, \alpha_v, \beta_u, \beta_v, \mu, \sigma, \gamma)'$ .

### 3.1.2 Tuberculosis transmission dynamics

The second model we consider was developed by Tanaka et al. (2006) for the study of tuberculosis transmission dynamics, and which has been used as a reference model for many subsequent ABC analyses (e.g. Fearnhead and Prangle, 2012; Sisson et al., 2007; Warne et al., 2018). The model describes the evolution of the number of tuberculosis cases,  $N(t)$ , over time given by

$$N(t) = \sum_{i=1}^{G(t)} X_i(t),$$

where  $G(t)$  is the number of unique genotypes of the tuberculosis bacterium at time  $t$  and  $X_i(t)$  is the number of cases caused by the  $i$ th genotype. The time-varying evolution of the  $X_i(t)$ 's is driven by a linear birth-death process with birth rate  $\alpha$  and death rate  $\delta$ . Additionally, mutation events occur at rate  $\tau$  in which new genotypes are created.

Given values for  $\alpha$ ,  $\delta$  and  $\tau$ , realisations of this process can be generated using the *Gillespie Direct Method* (Gillespie, 1977) with propensity functions,

$$a_b(X_i(t)) = \alpha X_i(t), \quad a_d(X_i(t)) = \delta X_i(t), \quad a_m(X_i(t)) = \tau X_i(t),$$

where  $a_b$ ,  $a_d$  and  $a_m$  are the birth, death and mutation propensities respectively. Note that in the event of a mutation, the dimension of the state vector  $\mathbf{X}(t) = [X_1(t), X_2(t), \dots, X_{G(t)}(t)]$  increases (equivalently,  $\mathbf{X}(t)$  may be treated as an element from a sequence space).

Tanaka et al. (2006) demonstrate the application of ABC methods to infer the three rate parameters  $\boldsymbol{\theta} = (\alpha, \delta, \tau)'$  for a real dataset of tuberculosis cases in San Francisco during the early 1990s that consists of 326 distinct genotypes. The summary statistics used were the number of distinct genotypes,  $g$ , and the genetic diversity,  $H$  (see Tanaka et al. (2006) for details).

## 3.2 Parallelisation and vectorisation opportunities

Given  $P$  CPU cores, the processes of i.i.d. sampling  $(\boldsymbol{\theta}^*, \mathcal{D}^*)$  from the joint prior predictive can be trivially divided between cores. For the toggle switch model (Equation (4)) it is reasonable to divide the workload evenly across cores since the number of floating point operations per model realisation is independent of the parameter values. Such a workload division is called a **static** schedule in the **OpenMP** standard. In a **static** schedule, each core will generate  $N_P = N/P$  prior predictive samples. For simplicity, we will assume that  $N_P$  is an integer.

For the tuberculosis model, generation of the prior predictive samples involves a discrete-state, continuous-time Markov process that is implemented with the Gillespie algorithm. As a result, the simulation times can vary wildly and a **static** schedule could result in a load imbalance between cores. As a result, the **guided** or **dynamic** scheduling schemes could perform better. In practice, we found that the overhead associated with load imbalance becomes relatively low for larger  $N$ . Furthermore, an early termination rule, as used in the Lazy ABC approach of Prangle (2016), would also further reduce this imbalance. We conclude a standard **static** distribution of prior predictive samples is appropriate as a general strategy for ABC applications.

Unfortunately, no such general strategy exists for vectorisation. The simulation algorithms for both ABC applications are very different. The toggle switch model utilises an Euler-Maruyama scheme, whereas the tuberculosis model utilises the Gillespie Direct method. Therefore we expect the performance improvement opportunity to differ.

A naïve, scalar implementation of the toggle switch model simulation would involve computing each realisation,  $u_i(T)$  for  $i = 1, 2, \dots, C$ , in sequence as shown in Algorithm 2.

Since each Euler-Maruyama simulation performs identical operations for each cell  $i = 1, 2, \dots, C$ , this is ideal for vectorisation. That is, we can evolve cells together in blocks of length  $V$  where  $64V$  is the bit width of the available VPU. Aside from the generation of Gaussian random variates, every operation in Algorithm 2 may be replaced with a element-wise vector operation. However, we generate  $2n_t V$  Gaussian variates using the high performing Intel MKL RNG prior to processing each block. This is efficient provided  $n_t V$  is small enough to fit into L1 cache, but large enough to take advantage of the Intel routines (typically the Intel routines require more than 1,000 variates to be generated in a

---

**Algorithm 2** Scalar implementation of Euler-Maruyama scheme for the toggle switch model

---

- 1: Initialise  $u_{i,0} \leftarrow u_0, v_{i,0} \leftarrow v_0$  for  $i = 1, 2, \dots, C$ ;
  - 2: Set  $n_t \leftarrow T/\Delta t$ ;
  - 3: **for**  $i = 1, 2, \dots, C$  **do**
  - 4:   **for**  $j = 0, 1, \dots, n_t - 1$  **do**
  - 5:     Generate increments  $\xi_{i,u}^j, \xi_{i,v}^j \sim \mathcal{N}(0, \Delta t)$ ;
  - 6:      $u_i^{j+1} \leftarrow u_i^j + \Delta t [\alpha_u / (1 + (v_i^j)^{\beta_u}) - 1 - 0.03u_i^j] + 0.5\xi_{i,u}^j$ ;
  - 7:      $v_i^{j+1} \leftarrow v_i^j + \Delta t [\alpha_v / (1 + (u_i^j)^{\beta_v}) - 1 - 0.03v_i^j] + 0.5\xi_{i,v}^j$ ;
  - 8:   **end for**
  - 9: **end for**
- 

block to attain peak performance).

The resulting vectorised Euler-Maruyama scheme is shown in Algorithm 3. Note the use

---

**Algorithm 3** Vectorised implementation of Euler-Maruyama scheme for the toggle switch model

---

- 1: Initialise  $u_{i,0} \leftarrow u_0, v_{i,0} \leftarrow v_0$  for  $i = 1, 2, \dots, C$ ;
  - 2: Set  $n_t \leftarrow T/\Delta t$ ;
  - 3: Set  $A_u \leftarrow \alpha_u \mathbf{e}_{1:V}$  and  $A_v \leftarrow \alpha_v \mathbf{e}_{1:V}$
  - 4: **for**  $i = 1, 1 + V, 1 + 2V, \dots, C + 1 - V, C$  **do**
  - 5:   Generate increments  $\xi_{i:i+V-1,u}^{0:n_t-1}, \xi_{i:i+V-1,v}^{0:n_t-1} \sim \mathcal{N}(0, \Delta t)$ ;
  - 6:   **for**  $j = 0, 1, \dots, n_t - 1$  **do**
  - 7:      $u_{i:i+V-1}^{j+1} \leftarrow u_{i:i+V-1}^j + \Delta t [A_u \oslash (\mathbf{e}_{1:V} + (u_{i:i+V-1}^j)^{\circ\beta_u}) - \mathbf{e}_{1:V} - 0.03u_{i:i+V-1}^j]$ ;
  - 8:      $u_{i:i+V-1}^{j+1} \leftarrow u_{i:i+V-1}^{j+1} + 0.5\xi_{i:i+V-1,u}^j$ ;
  - 9:      $v_{i:i+V-1}^{j+1} \leftarrow v_{i:i+V-1}^j + \Delta t [A_v \oslash (\mathbf{e}_{1:V} + (v_{i:i+V-1}^j)^{\circ\beta_v}) - \mathbf{e}_{1:V} - 0.03v_{i:i+V-1}^j]$ ;
  - 10:      $v_{i:i+V-1}^{j+1} \leftarrow v_{i:i+V-1}^{j+1} + 0.5\xi_{i:i+V-1,v}^j$ ;
  - 11:   **end for**
  - 12: **end for**
- 

of the notation “.” to mean a vector. For example e.g.,  $u_{i:i+V-1}^j = [u_i^j, u_{i+1}^j, \dots, u_{i+V-1}^j] \in \mathbb{R}^{1 \times V}$  and  $\xi_{i:i+V-1,u}^{0:n_t-1} = [\xi_{i,u}^0, \xi_{i+1,u}^0, \dots, \xi_{i+V-1,u}^0, \xi_{i,u}^1, \dots, \xi_{i+V-1,u}^{n_t-1}] \in \mathbb{R}^{n_t \times V}$ . Also denote  $\mathbf{e}_{1:V} = [1, 1, 1, \dots, 1] \in \mathbb{R}^{1 \times V}$ . We also use Hadamard notation for element-wise division,  $x \oslash y$ , multiplication,  $x \circ y$  and exponentiation,  $x^{\circ a}$ , where  $a$  is a scalar.

Unfortunately, there are fewer opportunities for vectorisation in the Gillespie method used in the tuberculosis model. The only suitable vectorisable step is in the calculation of genotype weights for the lookup method to select the genotype that will experience the next event. We can also vectorise the discrepancy measure components,  $g$ , and  $H$ . While this is not as significant as in the toggle switch model, the length of the state vector in the tuberculosis model is large enough that some performance boost from the vectorisation is still noticeable. The computation of the genetic diversity  $H$  is particularly efficient here due to the sum of squares operation that can exploit the fused-multiply-add VPU operations that performs  $A \leftarrow A + (B \circ C)$ .

Table 1: Computational performance of computing  $N = 4,000$  prior predictive samples under the toggle switch model using an Intel Xeon E5-2680v3 (Haswell) processor. Parallel times are based on 4-way multithreading and SIMD times using 256-bit vector operations.

Configuration		Runtime (Seconds) [Speedup factor]			
$C$	$T$	sequential	sequential+SIMD	parallel	parallel+SIMD
1,000	75	24.1 [1.0×]	7.2 [3.3×]	8.5 [2.8×]	4.0 [6.1×]
1,000	150	45.2 [1.0×]	11.4 [4.0×]	14.2 [3.2×]	5.0 [9.1×]
1,000	300	87.1 [1.0×]	20.3 [4.3×]	25.4 [3.4×]	7.1 [12.3×]
1,000	600	168.8 [1.0×]	37.2 [4.5×]	48.3 [3.5×]	11.5 [14.7×]
2,000	75	49.2 [1.0×]	14.9 [3.3×]	17.0 [2.9×]	7.93 [6.2×]
2,000	150	90.3 [1.0×]	23.4 [3.9×]	28.3 [3.2×]	10.1 [9.0×]
2,000	300	172.3 [1.0×]	39.8 [4.3×]	51.0 [3.4×]	14.1 [12.2×]
2,000	600	339.0 [1.0×]	74.6 [4.5×]	96.0 [3.5×]	22.9 [14.8×]
4,000	75	96.9 [1.0×]	29.2 [3.3×]	33.9 [2.9×]	15.6 [6.2×]
4,000	150	180.7 [1.0×]	45.6 [4.0×]	56.6 [3.2×]	19.8 [9.2×]
4,000	300	345.6 [1.0×]	79.9 [4.3×]	101.9 [3.4×]	28.5 [12.1×]
4,000	600	680.0 [1.0×]	149.3 [4.6×]	192.5 [3.5×]	45.2 [15.0×]
8,000	75	191.5 [1.0×]	58.1 [3.3×]	65.2 [2.9×]	31.0 [6.2×]
8,000	150	343.3 [1.0×]	87.0 [4.0×]	111.9 [3.1×]	38.0 [9.0×]
8,000	300	663.4 [1.0×]	153.5 [4.3×]	198.2 [3.4×]	54.7 [12.1×]
8,000	600	1,307.7 [1.0×]	286.2 [4.6×]	375.9 [3.5×]	88.3 [14.8×]

### 3.3 Performance

We now report the performance improvements obtained through vectorisation and multithreading. We test on two CPU architectures, the Xeon E5-2680v3 (Haswell)<sup>6</sup> and Xeon Gold 6140 (Skylake)<sup>7</sup>. The Xeon E5-2680v3 supports Intel’s AVX2 instruction set with 256-bit vector operations, and the Xeon Gold 6140 supports Intel’s AVX512 instruction set with 512-bit vector operations. The Xeon Gold series is a part of Intel’s latest Scalable processor family that inherits much of the VPU technology from the Intel Xeon Phi family.

For the toggle switch model,  $N$  prior predictive samples are generated for a range of different cell counts  $C$  and observation times  $T$ . We present the results for  $N = 4,000$  in Tables 1 (Xeon E5-2680v3) and 2 (Xeon Gold 6140). The tables compare the scalar sequential runtimes against vectorised sequential, scalar parallel and vectorised parallel. Note that for 256-bit VPUs the vectorised sequential code out-performs the scalar parallel code using four cores. Furthermore, the vectorisation also further boosts the performance of the parallel code. This is a clear example of the benefits of designing algorithms for SIMD along with multithreading.

We achieve nearly  $15\times$  speedup over scalar sequential code using only four cores and 256-bit vector operations on the Xeon E5-2680v3, and nearly  $19\times$  speedup when we move to 512-bit

<sup>6</sup><https://ark.intel.com/products/81908/Intel-Xeon-Processor-E5-2680-v3-30M-Cache-2-50-GHz->

<sup>7</sup><https://ark.intel.com/products/120485/Intel-Xeon-Gold-6140-Processor-24-75M-Cache-2-30-GHz->

Table 2: Computational performance of computing  $N = 4,000$  prior predictive samples under the toggle switch model using an Intel Xeon Gold 6140 (Skylake) processor. Parallel times are based on 4-way multithreading and SIMD times using 512-bit vector operations.

Configuration		Runtime (Seconds) [Speedup factor]			
$C$	$T$	sequential	sequential+SIMD	parallel	parallel+SIMD
1,000	75	21.0 [1.0×]	5.8 [3.6×]	7.1 [3.0×]	3.3 [6.4×]
1,000	150	38.9 [1.0×]	8.4 [4.6×]	11.7 [3.3×]	4.0 [9.8×]
1,000	300	75.2 [1.0×]	13.6 [5.5×]	20.8 [3.6×]	5.3 [14.2×]
1,000	600	148.9 [1.0×]	24.0 [6.2×]	39.0 [3.8×]	8.0 [18.7×]
2,000	75	41.9 [1.0×]	11.6 [3.6×]	14.3 [2.9×]	6.6 [6.4×]
2,000	150	78.0 [1.0×]	16.9 [4.6×]	23.3 [3.3×]	7.9 [9.8×]
2,000	300	150.1 [1.0×]	27.1 [5.5×]	41.6 [3.6×]	10.5 [14.3×]
2,000	600	294.5 [1.0×]	48.0 [6.1×]	77.9 [3.8×]	16.9 [17.5×]
4,000	75	83.9 [1.0×]	23.2 [3.6×]	28.5 [3.0×]	13.2 [6.4×]
4,000	150	156.3 [1.0×]	33.7 [4.6×]	46.7 [3.3×]	15.9 [9.9×]
4,000	300	300.2 [1.0×]	54.3 [5.5×]	82.9 [3.6×]	21.1 [14.2×]
4,000	600	588.9 [1.0×]	95.8 [6.1×]	155.5 [3.8×]	31.8 [18.5×]
8,000	75	167.9 [1.0×]	46.6 [3.6×]	57.0 [3.0×]	26.4 [6.4×]
8,000	150	311.9 [1.0×]	67.3 [4.6×]	93.2 [3.4×]	31.7 [9.8×]
8,000	300	600.5 [1.0×]	109.1 [5.5×]	165.9 [3.6×]	42.2 [14.2×]
8,000	600	1,180.7 [1.0×]	191.4 [6.2×]	311.6 [3.8×]	63.5 [18.6×]

vector operations on the Xeon Gold 6140. At a glance the step from  $15\times$  to  $19\times$  seems lower than expected when the vector units have doubled in width. Based on the numbers from the vectorised sequential versions the performance the Xeon E5-2680v3 attains a speedup factor that is 57% of perfect speedup, which is based on two 256-bit VPU, resulting in an  $8\times$  speedup if everything vectorises perfectly; an unrealistic scenario. For the Xeon Gold 6140, this reduces to about 40% of a perfect speedup of  $16\times$ . This is consistent with Amdahl’s law (Equation (2)) since both speedups correspond to  $8.4C_S = C_P$  which implies that even if all vectorised operations are computed instantaneously, the maximum performance improvement is about  $9.4\times$  from vectorisation alone.

Tables 3 (Xeon E5-2680v3) and 4 (Xeon Gold 6140) show the performance results for the tuberculosis model for a range of prior predictive sample counts,  $N$ . The speedup factor from vectorisation is unsurprisingly not as significant as for the toggle switch model. This is an important demonstration of the limitations of SIMD operations (this includes GPGPU-based accelerators). However, there is still improvement from vectorisation of between  $1.4\times$  to  $1.8\times$ , which is still good in the context of the HPC literature (Dongarra et al., 2014; Kozlov et al., 2014; Mudalige et al., 2016).

Interestingly, the speedup factor due to vectorisation is larger, at  $1.8\times$ , for the Xeon E5-2680v3 compared with  $1.4\times$  for the Xeon Gold 6140. However, the Xeon Gold 6140 results demonstrate almost  $3\times$  improvement in the scalar performance over the Xeon E5-2680v3. This was not observed in the toggle switch case. Therefore, we conclude that the tubercu-

Table 3: Computational performance of computing prior predictive samples under the tuberculosis model using an Intel Xeon E5-2680v3 (Haswell) processor. Parallel times are based on 4-way multithreading and SIMD times using 256-bit vector operations.

Number of samples $N$	Runtime (Seconds) [Speedup factor]			
	sequential	sequential+SIMD	parallel	parallel+SIMD
500	46.7 [1.0×]	25.5 [1.8×]	64.5 [0.7×]	36.0 [1.3×]
1,000	230.2 [1.0×]	127.7 [1.8×]	72.1 [3.2×]	40.1 [5.8×]
2,000	385.0 [1.0×]	212.7 [1.8×]	91.8 [4.2×]	50.8 [7.6×]
4,000	657.4 [1.0×]	363.1 [1.8×]	229.5 [2.9×]	127.7 [5.2×]
8,000	1,175.6 [1.0×]	649.2 [1.8×]	386.7 [3.0×]	212.5 [5.5×]
16,000	2,601.7 [1.0×]	1,449.4 [1.8×]	697.3 [3.7×]	389.6 [6.7×]

Table 4: Computational performance of computing prior predictive samples under the tuberculosis model using an Intel Xeon Gold 6140 (Skylake) processor. Parallel times are based on 4-way multithreading and SIMD times using 512-bit vector operations.

Number of samples $N$	Runtime (Seconds) [Speedup factor]			
	sequential	sequential+SIMD	parallel	parallel+SIMD
500	15.9 [1.0×]	11.5 [1.4×]	23.7 [0.7×]	17.9 [0.9×]
1,000	83.9 [1.0×]	61.5 [1.4×]	26.3 [3.2×]	19.3 [4.4×]
2,000	138.2 [1.0×]	101.2 [1.4×]	32.8 [4.2×]	24.0 [5.8×]
4,000	233.5 [1.0×]	170.7 [1.4×]	83.8 [2.8×]	61.5 [3.8×]
8,000	412.9 [1.0×]	301.9 [1.4×]	138.1 [3.0×]	101.1 [4.1×]
16,000	922.5 [1.0×]	675.2 [1.4×]	249.7 [3.7×]	183.0 [5.0×]

losis model simulation is accessing L3 cache and main memory more often, and thus taking advantage of the memory bandwidth and extra memory channels on the Xeon Gold 6140. If the tuberculosis model is not utilising L1 and L2 cache as intensively, this would also explain the reduced speedup from moving to wider vectors since the VPU cannot be kept busy.

The distinct difference in performance of the toggle switch model and the tuberculosis model suggests that care must be taken when choosing the stochastic simulation algorithm. For example, introducing approximations (Gillespie, 2000, 2001) for the tuberculosis model could significantly improve performance.

### 3.4 Summary

We have demonstrated that the utilisation of SIMD operations can improve the performance of prior predictive sampling for ABC by a factor of more than 6× compared with standard scalar implementations. In particular, we have highlighted that specific features of the stochastic model and simulation algorithm have a great impact on the potential improvements of SIMD operations. Simulation schemes such as Euler-Maruyama are ideal candidates for vectorisation, however, exact stochastic simulation methods like the Gille-

spie direct method are far more challenging. Regardless, a speedup of at least  $1.4\times$  was achieved through vectorisation, in this case.

## 4 Weakly informative priors

Our second application is the selection of weakly informative priors in Bayesian inference. We specifically focus on the computational approach of Nott et al. (2018), which is based on the theoretical framework of Evans and Jang (2011) and Gelman (2006).

### 4.1 Testing weak prior informativity

Following the work of Nott et al. (2018), we consider the prior predictive  $p$ -value,

$$p(\mathcal{D}_{\text{obs}}) = \mathbb{P} \left( \frac{1}{\pi(\mathcal{D})} \geq \frac{1}{\pi(\mathcal{D}_{\text{obs}})} \right) = \mathbb{P} (\pi(\mathcal{D}) \leq \pi(\mathcal{D}_{\text{obs}})), \quad (6)$$

as a measure of Bayesian model criticism, where  $\mathcal{D}_{\text{obs}}$  are the observational data, and  $\pi(\mathcal{D})$  is the prior predictive distribution (Equation (3)). Equation (6) provides a  $p$ -value for prior-data conflict (Evans and Jang, 2011; Nott et al., 2018) which occurs when the model parameters that result in a good fit with the data have low prior probability density. If  $\gamma$  is some pre-defined small cut-off, then  $p(\mathcal{D}_{\text{obs}}) \leq \gamma$  signifies prior-data conflict.

Suppose we have a family of priors,  $\pi(\boldsymbol{\theta} \mid \boldsymbol{\lambda})$ , that are parameterised by the hyperparameter  $\boldsymbol{\lambda} \in \boldsymbol{\Lambda}$ . Let the base prior, denoted by  $\pi(\boldsymbol{\theta} \mid \boldsymbol{\lambda}_0)$  for some  $\boldsymbol{\lambda}_0 \in \boldsymbol{\Lambda}$ , represent the current best knowledge of the parameter  $\boldsymbol{\theta}$ . Let

$$\pi(\mathcal{D} \mid \boldsymbol{\lambda}) = \int_{\boldsymbol{\theta}} \mathcal{L}(\boldsymbol{\theta}; \mathcal{D}) \pi(\boldsymbol{\theta} \mid \boldsymbol{\lambda}) \, \text{d}\boldsymbol{\theta} \quad (7)$$

be the prior predictive distribution for a given prior  $\pi(\boldsymbol{\theta} \mid \boldsymbol{\lambda})$  and let  $p_{\boldsymbol{\lambda}}(\mathcal{D}_{\text{obs}})$  be the prior predictive  $p$ -value under the prior  $\pi(\mathcal{D} \mid \boldsymbol{\lambda})$  (equivalent to Equation (6)),

$$p_{\boldsymbol{\lambda}}(\mathcal{D}_{\text{obs}}) = \mathbb{P} (\pi(\mathcal{D} \mid \boldsymbol{\lambda}) \leq \pi(\mathcal{D}_{\text{obs}} \mid \boldsymbol{\lambda})). \quad (8)$$

Assuming data that is generated under the base prior predictive distribution, that is,  $\mathcal{D}_0 \sim \pi(\mathcal{D} \mid \boldsymbol{\lambda}_0)$ , the task is to find values of  $\boldsymbol{\lambda}$  such that,

$$\mathbb{P} (p_{\boldsymbol{\lambda}}(\mathcal{D}_0) \leq \gamma) < \mathbb{P} (p_{\boldsymbol{\lambda}_0}(\mathcal{D}_0) \leq \gamma). \quad (9)$$

Priors that satisfy Equation (9) are called weakly informative with respect to the base prior. That is, weak informativity indicates less prior-data conflict than the base. Equivalently, weak informativity at level  $\alpha$  indicates that  $\gamma_{\boldsymbol{\lambda},\alpha} > \gamma_{\boldsymbol{\lambda}_0,\alpha}$  where  $\gamma_{\boldsymbol{\lambda},\alpha}$  and  $\gamma_{\boldsymbol{\lambda}_0,\alpha}$  are the prior-data conflict cut-offs such that  $\mathbb{P} (p_{\boldsymbol{\lambda}}(\mathcal{D}_0) \leq \gamma_{\boldsymbol{\lambda},\alpha}) = \mathbb{P} (p_{\boldsymbol{\lambda}_0}(\mathcal{D}_0) \leq \gamma_{\boldsymbol{\lambda}_0,\alpha}) = \alpha$ .

Therefore, given a set of  $K$  hyperparameter values,  $\boldsymbol{\lambda}_1, \dots, \boldsymbol{\lambda}_K \in \boldsymbol{\Lambda}$ , with  $\boldsymbol{\lambda}_0$  corresponding to the base prior, the task is to compute  $\gamma_{\boldsymbol{\lambda}_k,\alpha}$  such that  $\mathbb{P} (p_{\boldsymbol{\lambda}_k}(\mathcal{D}_0) \leq \gamma_{\boldsymbol{\lambda}_k,\alpha}) = \alpha$  for

$k = 0, 1, \dots, K$  and  $\mathcal{D}_0 \sim \pi(\mathcal{D} \mid \boldsymbol{\lambda}_0)$ . The high-level process proceeds as in Algorithm 4. The output of Algorithm 4 is a set of  $\alpha$  level cutoffs  $\{\gamma_{\boldsymbol{\lambda}_0, \alpha}, \gamma_{\boldsymbol{\lambda}_1, \alpha}, \dots, \gamma_{\boldsymbol{\lambda}_K, \alpha}\}$ , from which we can derive a set of weakly informative prior distributions with respect to the base prior  $\pi(\boldsymbol{\theta} \mid \boldsymbol{\lambda}_0)$ , that is,  $\{\pi(\boldsymbol{\theta} \mid \boldsymbol{\lambda}_k) : \gamma_{\boldsymbol{\lambda}_k, \alpha} > \gamma_{\boldsymbol{\lambda}_0, \alpha}, k = 1, 2, \dots, K\}$ .

---

**Algorithm 4** Weak informativity test

---

```

1: Initialise hyperparameters  $\boldsymbol{\lambda}_0, \boldsymbol{\lambda}_1, \dots, \boldsymbol{\lambda}_K \in \boldsymbol{\Lambda}$ , with base parameter  $\boldsymbol{\lambda}_0$ ;
2: for  $k \in [0, 1, \dots, K]$  do
3:   for  $i \in [1, 2, \dots, N]$  do
4:     Generate data from base prior predictive  $\mathcal{D}_0^{(i)} \sim \pi(\mathcal{D} \mid \boldsymbol{\lambda}_0)$ ;
5:     Generate data from prior predictive  $\mathcal{D}_k^{(i)} \sim \pi(\mathcal{D} \mid \boldsymbol{\lambda}_k)$ ;
6:     Evaluate  $\pi_0^i \leftarrow \pi(\mathcal{D}_0^{(i)} \mid \boldsymbol{\lambda}_k)$  and  $\pi_k^i \leftarrow \pi(\mathcal{D}_k^{(i)} \mid \boldsymbol{\lambda}_k)$ ;
7:   end for
8:   for  $i \in [1, 2, \dots, N]$  do
9:     Estimate  $p$ -value samples  $p_k^i \leftarrow p_{\boldsymbol{\lambda}_k}(\mathcal{D}_0^{(i)}) \approx \frac{1}{N} \sum_{j=1}^N \mathbb{1}_{[0, \pi_0^i]}(\pi_k^j)$ ;
10:  end for
11:  Compute  $\gamma_{\boldsymbol{\lambda}_k, \alpha}$  as the  $\alpha$  quantile of  $\{p_k^1, p_k^2, \dots, p_k^N\}$ ;
12: end for

```

---

This is an extremely computationally intensive task since the normalising constant of the posterior density,  $\pi(\mathcal{D} \mid \boldsymbol{\lambda})$ , must be evaluated for many different  $\mathcal{D}$ . Here we use an adaptive sequential Monte Carlo (SMC) sampler using likelihood annealing and a Markov chain Monte Carlo (MCMC) proposal kernel (Beskos et al., 2016; Chopin, 2002; Drovandi and Pettitt, 2011) to estimate the normalising constant. This SMC sampler is given in Algorithm 5. Algorithm 4 requires  $2KN$  executions of the adaptive SMC (Algorithm 5) with  $N_p$  particles and appropriate tuning parameters  $c$ , related to the number of MCMC iterations, and  $h$ , related to the covariance of the Gaussian random walk MCMC proposals.

Just as in Evans and Jang (2011) and Nott et al. (2018), we consider weakly informative priors for the analysis of an acute toxicity test in which  $M$  groups of animals are given different dosages of some toxin, and the number of deaths in each group are recorded. A logistic regression model is applied for the number of deaths  $y_i$  in group  $i \in [1, 2, \dots, M]$ ,

$$y_i \sim \text{Bin} \left( n_i, \frac{1}{1 + e^{\beta_0 + \beta_1 x_i}} \right), \quad i = 1, 2, \dots, M, \quad (10)$$

where  $n_i$  and  $x_i$  are respectively the number of animals and the toxin dose level in the  $i$ th group, and model parameters are  $\boldsymbol{\theta} = (\beta_0, \beta_1)'$ . Given data  $\mathcal{D}_{\text{obs}} = [y_{\text{obs},1}, y_{\text{obs},2}, \dots, y_{\text{obs},M}]$ , the likelihood function is

$$\mathcal{L}(\boldsymbol{\theta}; \mathcal{D}_{\text{obs}}) = \prod_{i=1}^M \binom{n_i}{y_{\text{obs},i}} \left( \frac{1}{1 + e^{\beta_0 + \beta_1 x_i}} \right)^{y_{\text{obs},i}} \left( 1 - \frac{1}{1 + e^{\beta_0 + \beta_1 x_i}} \right)^{n_i - y_{\text{obs},i}}. \quad (11)$$

We consider the family of bivariate Gaussian priors of the form,  $\boldsymbol{\theta} \sim \mathcal{N}(\mathbf{0}, \text{diag}(\boldsymbol{\lambda})^2)$  with hyperparameter vector  $\boldsymbol{\lambda}$ . For our specific implementation we have  $M = 4$ ,  $n_1 = n_2 =$

---

**Algorithm 5** SMC sampler using  $N_p$  particles for estimating  $\pi(\mathcal{D} \mid \boldsymbol{\lambda})$ 


---

- 1: Initialise  $n = 0$ ,  $t_0 = 0$ ,  $\pi_0(\mathcal{D} \mid \boldsymbol{\lambda}) = 1$ ,  $\boldsymbol{\theta}_0^{(i)} \sim \pi(\boldsymbol{\theta} \mid \boldsymbol{\lambda})$ , and  $W_0^{(i)} = 1/N_p$  for  $i = 1, 2, \dots, N_p$ , and specify user-defined values for tuning parameters  $h$  and  $c$ ;
  - 2: **repeat**
  - 3:   Set  $n \leftarrow n + 1$ ;
  - 4:   Find  $t$  such that  $\left[ \sum_{i=1}^{N_p} \left( \frac{W_{n-1}^{(i)} \mathcal{L}(\boldsymbol{\theta}_{n-1}^{(i)}; \mathcal{D})^{t_n - t_{n-1}}}{\sum_{j=1}^{N_p} W_{n-1}^{(j)} \mathcal{L}(\boldsymbol{\theta}_{n-1}^{(j)}; \mathcal{D})^{t_n - t_{n-1}}} \right)^2 \right]^{-1} = N_p/2$ , that is, the effective sample size (ESS) is  $N_p/2$ ; Set  $t_n \leftarrow \min(1, t)$ ;
  - 5:   Set  $W_n^{(i)} \leftarrow W_{n-1}^{(i)} \mathcal{L}(\boldsymbol{\theta}_{n-1}^{(i)}; \mathcal{D})^{t_n - t_{n-1}}$  for  $i = 1, 2, \dots, N_p$ ;
  - 6:   Set  $\pi_n(\mathcal{D} \mid \boldsymbol{\lambda}) = \pi_{n-1}(\mathcal{D} \mid \boldsymbol{\lambda}) \left[ \frac{1}{N_p} \sum_{i=1}^{N_p} \mathcal{L}(\boldsymbol{\theta}_{n-1}^{(i)}; \mathcal{D})^{t_n - t_{n-1}} \right]$
  - 7:   Resample with replacement the particles  $\boldsymbol{\theta}_n^{(i)} \sim \{\boldsymbol{\theta}_n^{(j)}, W_n^{(j)}\}_{j=1}^{N_p}$  for  $i = 1, 2, \dots, N_p$ ;
  - 8:   Set  $W_n^{(i)} \leftarrow 1/N_p$  for  $i = 1, 2, \dots, N_p$ ;
  - 9:   Construct a tuned proposal kernel  $q(u \mid v) = \phi(u; v, h^2 \hat{\Sigma}_n)$ , where  $\hat{\Sigma}_n$  is the sample covariance matrix computed using  $\{\boldsymbol{\theta}_n^{(j)}\}_{j=1}^{N_p}$ ;
  - 10:   Set  $R_n \leftarrow \lceil \frac{\ln c}{\ln(1 - p_{\text{acc}})} \rceil$  where  $p_{\text{acc}}$  is the estimated acceptance probability determined from initial trial MCMC iterations and  $\lceil \cdot \rceil$  is the ceiling function;
  - 11:   **for**  $i \in [1, 2, \dots, N_p]$  **do**
  - 12:     **for**  $r = 1, 2, \dots, R_n$  **do**
  - 13:       Generate proposal  $\boldsymbol{\theta}^* \sim q(\boldsymbol{\theta} \mid \boldsymbol{\theta}_n^{(i)})$
  - 14:       Compute acceptance ratio,  $\alpha(\boldsymbol{\theta}^*, \boldsymbol{\theta}_n^{(i)}) \leftarrow \frac{\mathcal{L}(\boldsymbol{\theta}^*; \mathcal{D})^{t_n} \pi(\boldsymbol{\theta}^* \mid \boldsymbol{\lambda}) q(\boldsymbol{\theta}_n^{(i)} \mid \boldsymbol{\theta}^*)}{\mathcal{L}(\boldsymbol{\theta}_n^{(i)}; \mathcal{D})^{t_n} \pi(\boldsymbol{\theta}_n^{(i)} \mid \boldsymbol{\lambda}) q(\boldsymbol{\theta}^* \mid \boldsymbol{\theta}_n^{(i)})}$
  - 15:       With probability  $\min(1, \alpha(\boldsymbol{\theta}^*, \boldsymbol{\theta}_n^{(i)}))$ , set  $\boldsymbol{\theta}_n^{(i)} \leftarrow \boldsymbol{\theta}^*$ ;
  - 16:     **end for**
  - 17:   **end for**
  - 18: **until**  $t_n = 1$
- 

$n_3 = n_4 = 5$ ,  $x_1 = -0.86$ ,  $x_2 = -0.3$ ,  $x_3 = -0.05$  and  $x_4 = -0.75$ . The base prior hyperparameters are  $\boldsymbol{\lambda}_0 = (10, 2.5)'$ .

## 4.2 Parallelisation and vectorisation opportunities

There are many parallel implementations of SMC samplers using multithreading, however the resampling step and annealing both require thread synchronisation (Hurn et al., 2016; Lee et al., 2010; Murray et al., 2016). Consequently, it is more beneficial in our case to distribute the  $K$  hyperparameter values in Algorithm 4 across  $P$  cores, with each thread computing the  $\alpha$  quantile for  $K_P = K/P$  hyperparameters, since these may be performed completely independently. For every hyperparameter, we sequentially process the  $N$   $p$ -value computations. We focus on acceleration of the SMC sampler (Algorithm 5) through vectorisation.

In many ways, SMC samplers are well suited to vectorisation since synchronisation is ef-

fectively maintained automatically. While there are many aspects of Algorithm 5 that we vectorise in the code examples, we focus here on the vectorisation of the MCMC proposal kernel for diversification of particles (Steps 11–17 of Algorithm 5) as it has the greatest effect on performance improvements.

The strategy we employ is similar to the vectorisation of the Euler-Maruyama scheme (Algorithm 3) as presented in Section 3 for the toggle switch model. At SMC step  $n$ , each particle is perturbed via  $R_n$  MCMC steps. The same operations are performed at each MCMC iteration, with the exception of a single branch operation that arises from the accept/reject step. Therefore, we process the particle updates in blocks of length  $V$  and evolve the  $R_n$  MCMC steps for this block together using vector operations. Just as with the Euler-Maruyama scheme, all of the Gaussian and uniform random variates required for the block are generated together before the block is processed. We use the same vector notation as in Section 3, however, we also define the element-wise application of a function,  $f$ , over vectors of length  $V$  using the notation  $f^V(x_{i:i+V}) = [f(x_i), f(x_{i+1}), \dots, f(x_{i+V})]$ . The vectorised MCMC proposals are performed as in Algorithm 6.

---

**Algorithm 6** Vectorised implementation of MCMC proposals for SMC

---

```

1: for  $i = 1, 1 + V, 1 + 2V, \dots, N_p + 1 - V, N_p$  do
2:   Generate increments  $\xi_{1:V}^{1:R_n} \sim \mathcal{N}(\mathbf{0}, h\hat{\Sigma})$ ;
3:   Generate uniform variates  $u_{1:V}^{1:R_n} \sim \mathcal{U}(0, 1)$ ;
4:   for  $r = 1, 2, \dots, R_n$  do
5:     Generate proposal  $\theta_{1:V}^* \leftarrow \theta_n^{(i:i+V)} + \xi_{1:V}^r$ ;
6:      $\alpha_{1:V} \leftarrow \mathcal{L}^V(\theta_{1:V}^*; \mathcal{D})^{\circ t_n} \circ \pi^V(\theta_{1:V}^* | \lambda) \circ \phi^V(\theta_n^{(i:i+V)}; \theta_{1:V}^*, h\hat{\Sigma})$ ;
7:      $\alpha_{1:V} \leftarrow \alpha_{1:V} \odot \left[ \mathcal{L}^V(\theta_n^{(i:i+V)}; \mathcal{D})^{\circ t_n} \circ \pi^V(\theta_n^{(i:i+V)} | \lambda) \circ \phi^V(\theta_n^{(i:i+V)}; \theta_n^{(i:i+V)}, h\hat{\Sigma}) \right]$ ;
8:     for  $j = 1, 2, \dots, V$  do
9:       if  $u_j^r \leq \alpha_j$  then
10:         $\theta_n^{(i:i+j-1)} \leftarrow \theta_j^*$ ;
11:       end if
12:     end for
13:   end for
14: end for

```

---

In practice, Algorithm 6 works with the likelihood and prior on the log scale to avoid numerical underflow, however we present the direct implementation here for clarity. Also, while we represent the accept/reject step as a loop using scalar operations, in reality, the conditional statement is also vectorised in our example codes. However, the accept/reject step is not a significant computational portion of the algorithm. For optimal performance, it is essential that we have vectorised forms of the likelihood  $\mathcal{L}^V$ , the prior density  $\pi^V$  and the Gaussian proposal density  $\phi^V$ . This is quite straight forward for the logistic regression model and for the Gaussian priors and proposals used in this example.

Other aspects of Algorithm 5 that could be vectorised include likelihood evaluations and the computation of ESS and weight updates. The main scalar bottleneck is the resampling step that involves sampling from a multinomial distribution via the look-up method.

Parallel approximations for resampling have been proposed (Murray et al., 2016) and these techniques have been demonstrated to be very effective for large scale SMC samplers. However, since we focus here on a SIMD implementation of SMC, we have not implemented this approach. Extending the ideas of Murray et al. (2016) to the SIMD paradigm we consider an important piece of future work.

### 4.3 Performance

We test the performance improvement obtained through vectorisation and multithreading using the Xeon E5-2680v3 and Xeon Gold 6140 processors. The evaluation of the weak informativity test in Algorithm 4 is performed for a range of values for  $K$ , the number of hyperparameters, and  $N$  the number of datasets. In all simulations, the  $K$  hyperparameter values are generated using a bivariate uniform distribution  $\boldsymbol{\lambda}_k \sim \mathcal{U}([0.1, 10] \times [0.1, 20])$  for  $k = 1, 2, \dots, K$ . The SMC sampling is performed with  $N_p = 500$  particles, with the lower particle count enabling computation to remain largely within L1 and L2 cache. Tuning parameter values are specified as  $c = 0.01$  and  $h = 2.38/\sqrt{2}$ . Results are provided in Tables 5 and 6.

Across all configurations, a consistent improvement due to vectorisation of  $2.1\times$  is achieved using the Xeon E5-2680v3 and  $2.3\times$  when using the Xeon Gold 6140. Once again, diminishing returns are observed when stepping from 256-bit vector operations to 512-bit vector operations.

It is worth noting that, in our bioassay example, the MCMC proposal kernel performs a small number of MCMC steps (usually no more than  $R_n = 30$ ) and the number of particles in the SMC sampler is  $N_p = 500$ . In Tables 1 and 2, the overall performance boost increases with larger  $T$  and  $C$ . Therefore, we expect the overall performance improvement to increase in cases when longer MCMC runs are required, since the MCMC step will dominate each SMC iteration and more efficient reuse of L1 cache data will be achieved.

Table 5: Computational performance of the weak informativity test using an Intel Xeon E5-2680v3 (Haswell) processor. Parallel times are based on 4-way multithreading and SIMD times using 256-bit vector operations.

Configuration		Runtime (Seconds) [Speedup factor]			
$N$	$K$	sequential	sequential+SIMD	parallel	parallel+SIMD
50	50	46.1 [1.0×]	22.3 [2.1×]	11.6 [4.0×]	5.87 [7.9×]
100	50	92.6 [1.0×]	44.8 [2.1×]	23.2 [4.0×]	11.41 [8.1×]
200	50	184.6 [1.0×]	89.2 [2.1×]	46.5 [4.0×]	22.89 [8.1×]
400	50	370.7 [1.0×]	179.0 [2.1×]	92.8 [4.0×]	45.75 [8.1×]
50	100	90.91 [1.0×]	44.0 [2.1×]	22.9 [4.0×]	11.18 [8.1×]
100	100	181.4 [1.0×]	87.7 [2.1×]	45.3 [4.0×]	22.14 [8.2×]
200	100	364.3 [1.0×]	175.6 [2.1×]	91.1 [4.0×]	44.28 [8.2×]
400	100	728.4 [1.0×]	351.9 [2.1×]	181.7 [4.0×]	88.80 [8.2×]
50	200	181.0 [1.0×]	87.5 [2.1×]	45.0 [4.0×]	21.94 [8.3×]
100	200	362.4 [1.0×]	175.7 [2.1×]	89.8 [4.0×]	43.84 [8.3×]
200	200	723.8 [1.0×]	350.7 [2.1×]	179.3 [4.0×]	88.55 [8.2×]
400	200	1,451.6 [1.0×]	701.7 [2.1×]	358.1 [4.1×]	175.90 [8.3×]
50	400	362.3 [1.0×]	175.0 [2.1×]	89.4 [4.1×]	43.90 [8.3×]
100	400	723.6 [1.0×]	349.9 [2.1×]	179.5 [4.0×]	87.61 [8.3×]
200	400	1,446.6 [1.0×]	701.9 [2.1×]	358.0 [4.0×]	175.27 [8.3×]
400	400	2,898.9 [1.0×]	1,400.9 [2.1×]	715.6 [4.1×]	349.83 [8.3×]

Table 6: Computational performance of the weak informativity test using an Intel Xeon Gold 6140 (Skylake) processor. Parallel times are based on 4-way multithreading and SIMD times using 512-bit vector operations.

Configuration		Runtime (Seconds) [Speedup factor]			
$N$	$K$	sequential	sequential+SIMD	parallel	parallel+SIMD
50	50	45.9 [1.0×]	21.0 [2.2×]	11.7 [3.9×]	5.7 [8.0×]
100	50	95.0 [1.0×]	42.1 [2.3×]	23.9 [4.0×]	10.8 [8.8×]
200	50	189.3 [1.0×]	84.0 [2.3×]	47.8 [4.0×]	21.6 [8.8×]
400	50	378.3 [1.0×]	167.7 [2.3×]	93.8 [4.0×]	43.2 [8.8×]
50	100	89.6 [1.0×]	41.3 [2.2×]	22.7 [4.0×]	10.6 [8.4×]
100	100	186.1 [1.0×]	82.8 [2.3×]	46.5 [4.00×]	21.1 [8.8×]
200	100	372.5 [1.0×]	165.7 [2.3×]	92.9 [4.0×]	42.2 [8.8×]
400	100	749.1 [1.0×]	331.9 [2.3×]	183.9 [4.1×]	84.6 [8.9×]
50	200	178.6 [1.0×]	82.3 [2.2×]	43.8 [4.1×]	20.8 [8.6×]
100	200	372.5 [1.0×]	165.0 [2.3×]	90.7 [4.1×]	42.1 [8.8×]
200	200	744.4 [1.0×]	330.4 [2.3×]	181.4 [4.1×]	84.0 [8.9×]
400	200	1,489.5 [1.0×]	660.7 [2.3×]	359.5 [4.1×]	167.9 [8.9×]
50	400	357.5 [1.0×]	165.1 [2.2×]	89.4 [4.0×]	41.9 [8.5×]
100	400	745.6 [1.0×]	330.4 [2.3×]	184.4 [4.0×]	83.4 [8.9×]
200	400	1,489.5 [1.0×]	661.0 [2.3×]	369.0 [4.0×]	167.4 [8.9×]
400	400	2,982.6 [1.0×]	1,323.8 [2.3×]	728.3 [4.1×]	335.3 [8.9×]

## 4.4 Summary

We have presented the challenging problem of weak informativity tests over a family of priors  $\pi(\boldsymbol{\theta} \mid \boldsymbol{\lambda})$  with respect to a base prior  $\pi(\boldsymbol{\theta} \mid \boldsymbol{\lambda}_0)$ . This requires a large number of approximations of the posterior normalising constant for different datasets from the prior predictive distribution, each of which is computationally challenging in its own right. The traditional approach of parallelisation of each SMC iteration would reduce the level of parallelism available across hyperparameters. Using a novel vectorised SMC implementation, we double our computational performance and can reserve multithreading across hyperparameters, requiring very little thread communication. Of course, a combination of parallelism and vectorisation could be implemented to improve the performance of a single SMC step, however, in the context of weak informativity, this offers little benefit since utilising threads for SMC forces hyperparameters to be processed serially. If HPC resources are available then hyperparameters could be distributed across servers, and both threading and vectorisation in the SMC steps.

## 5 Parameter inference for a non-Gaussian asymmetric volatility model

For our last example, we apply an adaptive sequential Monte Carlo sampler to perform parameter inference in eleven dimensions for the “bad environment – good environment” (BEGE) model of innovations on stock market returns (Bekaert et al., 2015; Li et al., 2019; South et al., 2019).

### 5.1 The BEGE model

The BEGE model of Bekaert et al. (2015) is a non-Gaussian generalisation of the Glosten-Jagannathan-Runkle (GJR) asymmetric volatility model (Glosten et al., 1993) and is in the class of generalised autoregressive conditional heteroskedasticity (GARCH) models (Bollerslev, 1986; Engle, 1982). The BEGE model describes the time-series of stock market returns,  $\{r_t\}_{t \geq 0}$  using a model on innovation on returns,  $\{u_t\}_{t \geq 0}$ , that consists of a linear combination of “good environment” shocks,  $\{\omega_{p,t}\}_{t \geq 0}$ , and “bad environment” shocks,  $\{\omega_{n,t}\}_{t \geq 0}$ . The BEGE time-series evolves according to

$$\begin{aligned} r_{t+1} &= u_{t+1} + \mu, \\ u_{t+1} &= \sigma_p \omega_{p,t+1} - \sigma_n \omega_{n,t+1}, \\ \omega_{p,t+1} &\sim \tilde{\Gamma}(p_t, 1), \\ \omega_{n,t+1} &\sim \tilde{\Gamma}(n_t, 1), \end{aligned} \tag{12}$$

where  $\mu$  is the conditional mean of returns,  $\tilde{\Gamma}(k, \theta)$  is the centered (de-means) gamma distribution with shape,  $k$ , and scale,  $\theta$ . Thus,  $\{p_t\}_{t \geq 0}$  and  $\{n_t\}_{t \geq 0}$  are, respectively, the

shapes of the good and bad environment shocks. These shape parameters evolve according to

$$\begin{aligned} p_t &= p_0 + \rho_p p_{t-1} + \frac{\phi_p^+}{2\sigma_p^2} u_t^2 \mathbb{1}_{[0,\infty)}(u_t) + \frac{\phi_p^-}{2\sigma_p^2} u_t^2 \mathbb{1}_{(-\infty,0)}(u_t), \\ n_t &= n_0 + \rho_n n_{t-1} + \frac{\phi_n^+}{2\sigma_n^2} u_t^2 \mathbb{1}_{[0,\infty)}(u_t) + \frac{\phi_n^-}{2\sigma_n^2} u_t^2 \mathbb{1}_{(-\infty,0)}(u_t), \end{aligned} \quad (13)$$

where  $\mathbb{1}_A(x) = 1$  if  $x \in A$ , otherwise  $\mathbb{1}_A(x) = 0$ .

We use S&P Composite Index returns data to perform parameter inference on the unknown parameters in the BEGE model,  $\boldsymbol{\theta} = (p_0, \sigma_p, \rho_p, \phi_p^+, \phi_p^-, n_0, \sigma_n, \rho_n, \phi_n^+, \phi_n^-, \mu)'$ . Our data consists of  $T$  months of logged monthly divided-adjusted returns,  $\mathcal{D}_{\text{obs}} = R_{\text{obs},T} = \{r_{\text{obs},t}\}_{0 \leq t \leq T}$ . Vague priors are used with  $p_0 \sim \mathcal{U}(10^{-4}, 0.5)$ ,  $\sigma_p \sim \mathcal{U}(10^{-4}, 0.3)$ ,  $\rho_p \sim \mathcal{U}(10^{-4}, 0.99)$ ,  $\phi_p^+ \sim \mathcal{U}(10^{-4}, 0.5)$ ,  $\phi_p^- \sim \mathcal{U}(10^{-4}, 0.5)$ ,  $n_0 \sim \mathcal{U}(10^{-4}, 1)$ ,  $\sigma_n \sim \mathcal{U}(10^{-4}, 0.3)$ ,  $\rho_n \sim \mathcal{U}(10^{-4}, 0.99)$ ,  $\phi_n^+ \sim \mathcal{U}(-0.2, 0.1)$ ,  $\phi_n^- \sim \mathcal{U}(10^{-4}, 0.75)$ , and  $\mu \sim \mathcal{U}(-0.9, 0.9)$ .

The most significant computational challenge in this inference problem is the computational cost associated with the evaluation of the log-likelihood function,

$$\log \mathcal{L}(\boldsymbol{\theta}; \mathcal{D}_{\text{obs}}) = \log \mathcal{L}(\boldsymbol{\theta}; R_{\text{obs},T}) = \sum_{t=1}^T \log \pi(r_{\text{obs},t} \mid r_{\text{obs},t-1}, \boldsymbol{\theta}). \quad (14)$$

Evaluation of the transitional densities,  $\pi(r_{\text{obs},t} \mid r_{\text{obs},t-1}, \boldsymbol{\theta})$ , requires the BEGE density  $\pi_{\text{BEGE}}(u_t \mid \sigma_p, \sigma_n, p_{t-1}, n_{t-1})$ . This can be approximated by first computing the BEGE cumulative distribution function and then taking a finite difference approximation (Bekaert et al., 2015). The BEGE cumulative distribution function is given by,

$$F_{\text{BEGE}}(u_t \mid \sigma_p, \sigma_n, p_{t-1}, n_{t-1}) = \int_{-\infty}^{\infty} G_{\bar{\Gamma}}(\omega_{p,t} - u_t \mid n_{t-1}, \sigma_n) \pi_{\bar{\Gamma}}(\omega_{p,t} \mid p_{t-1}, \sigma_p) d\omega_{p,t}, \quad (15)$$

with  $G_{\bar{\Gamma}}(\omega_{p,t} - u_t \mid n_{t-1}, \sigma_n) = 1 - F_{\bar{\Gamma}}(\omega_{p,t} - u_t \mid n_{t-1}, \sigma_n)$ , where  $\pi_{\bar{\Gamma}}(\cdot \mid k, \theta)$  and  $F_{\bar{\Gamma}}(\cdot \mid k, \theta)$  are, respectively, the probability density and cumulative distribution functions of a centered gamma distribution with shape,  $k$ , and scale,  $\theta$ . The integral in Equation (15) can be approximated numerically using quadrature on a discretisation of the  $\omega_{p,t}$  parameter space. At each discretisation point we require two evaluations of the incomplete gamma function,

$$P(a, x) = \frac{1}{\Gamma(a)} \int_0^x e^{-t} t^{a-1} dt, \quad (16)$$

where  $\Gamma(a)$  is the gamma function. Equation (16) can be computed using a power series, however, the number of terms in the series required for convergence depends on the value of  $x$  (Press et al., 1992).

We apply an adaptive SMC sampler to move  $N_p$  particles from the prior  $\pi(\boldsymbol{\theta})$  to the posterior  $\pi(\boldsymbol{\theta} \mid R_{\text{obs},T})$  under the BEGE model. This is a very similar SMC sampler to that applied in Section 4 (Algorithm 5). The only major difference in this case is the selection of the scaling rule for the proposal kernel within the MCMC step. In this model,

the posterior is highly non-Gaussian, so we apply the method of Salomone et al. (2018) to evaluate a set of MCMC trials each with a random scale factor,  $h \in [0.1, 0.2, \dots, 1.0]$ , at each SMC iteration. We then choose the scale factor,  $h_{\text{opt}}$ , that maximises the median expected squared jump distance (Pasarica and Gelman, 2010) across all particles. The MCMC proposal process continues until the Markov chains for at least half of the SMC particles have moved further than this median (Salomone et al., 2018).

## 5.2 Parallelisation and vectorisation opportunities

In Section 4 we vectorised the MCMC proposal step in the SMC sampler, but used thread parallelism to run independent SMC samplers for different values of the hyperparameters. In the BEGE model inference problem, we would like to utilise both vectorisation and parallelism to accelerate a single SMC sampler.

As previously mentioned, parallel implementations have been well studied in the literature (Hurn et al., 2016; Lee et al., 2010; Murray et al., 2016). Within a single SMC iteration, particle operations are completely independent of each other. However, as we noted in Section 4, there is also automatic synchronisation occurring within the MCMC proposal mechanism. Therefore, rather than distribute  $N_p$  particles across  $P$  cores, we ensure that the distribute occurs in contiguous blocks of length  $V$ . That is, each core will process  $N_p/(PV)$  blocks of particles; again, for simplicity, we assume  $PV$  divides  $N_p$ . By ensuring all data associated with particles is processed in contiguous blocks for length  $V$ , we allow each thread to independently exploit a vectorised MCMC proposal mechanism similar to Algorithm 6.

Another way the vector operations are exploited is in the evaluation of the BEGE log-likelihood. Specifically, we vectorise the numerical approximation of the integral in Equation (15). Consider a discretisation of  $\omega_{p,t}$  using  $N_\omega + 1$  nodes with uniform spacing  $\Delta\omega$ . Then Equation (15) can be approximated by,

$$F_{\text{BEGE}}(u_t \mid \sigma_p, \sigma_n, p_{t-1}, n_{t-1}) \approx \sum_{j=1}^{N_\omega} \left\{ \left[ 1 - P \left( n_{t-1}, \frac{\omega_{p,t}^{j-1} - u_t + n_{t-1}\sigma_n}{\sigma_n} \right) \right] \right. \\ \left. \times \left[ P \left( p_{t-1}, \frac{\omega_{p,t}^j + p_{t-1}\sigma_p}{\sigma_p} \right) - P \left( p_{t-1}, \frac{\omega_{p,t}^{j-1} + p_{t-1}\sigma_p}{\sigma_p} \right) \right] \right\}, \quad (17)$$

where  $\omega_{p,t}^j = \omega_{p,t}^0 + j\Delta\omega$ , for  $j = 0, 1, \dots, N_\omega$  and  $\omega_{p,t}^0$  is the lower bound of the discretisation. Essentially for every point  $\{\omega_{p,t}^j\}_{0 \leq j \leq N_\omega}$  we must evaluate the incomplete gamma function twice; once with the  $p_{t-1}$  shape parameter and once with the  $n_{t-1}$  shape parameter. Therefore, we can consider efficiently vectorising the incomplete gamma function for blocks of  $\omega_{p,t}$  points of length  $V$ , that is, we require a function of the form  $P^V(a, x_{1:V}) = [P(a, x_1), P(a, x_2), \dots, P(a, x_V)]$ . We can achieve this by extending the method described in Press et al. (1992), resulting in the element-wise vector series expres-

sion,

$$\begin{aligned}
P^V(a, x_{1:V}) = & \left[ (\exp^V(-x_{1:V}) \circ (x_{1:V})^{\circ a}) \oslash (\Gamma(a)\mathbf{e}_{1:V}) \right] \\
& \circ \left[ \sum_{n=0}^{\infty} ((x_{1:V})^{\circ n}) \oslash ((n+1)\mathbf{e}_{1:V}) \right]
\end{aligned} \tag{18}$$

where  $\exp^V(-x_{1:V}) = [e^{-x_1}, e^{-x_2}, \dots, e^{-x_V}] \in \mathbb{R}^{1 \times V}$ . The structure of Equation (18) allows efficient iteration that reuses previous steps, thus enabling good use of L1 and L2 cache. Of course, the series must be truncated once the vector series has converged in terms of the  $\infty$ -norm.

Therefore, we proceed to approximate  $F_{\text{BEGE}}(u_t \mid \sigma_p, \sigma_n, p_{t-1}, n_{t-1})$  by: 1) applying Equation (18) across the discretisation,  $\{\omega_{p,t}^j\}_{0 \leq j \leq N_\omega}$ , in blocks of length  $V$  with shape parameter  $p_{t-1}$ ; 2) applying Equation (18) across the discretisation,  $\{\omega_{p,t}^j\}_{0 \leq j \leq N_\omega}$ , in blocks of length  $V$  with shape parameter  $n_{t-1}$ ; and accumulating the sum of products in Equation (17) efficiently using fused-multiply-add vector operations.

### 5.3 Performance

We test the performance improvement obtained through vectorisation and multithreading using the Xeon E5-2680v3 and Xeon Gold 6140 processors. The evaluation of the BEGE inference problem is performed using adaptive SMC with likelihood annealing over a range of particle population sizes  $N_p$ . In all simulations, we approximate  $F_{\text{BEGE}}(u_t \mid \sigma_p, \sigma_n, p_{t-1}, n_{t-1})$  using Equations (17) and (18) with the discretisation  $\{\omega_{p,t}^j\}_{0 \leq j \leq N_\omega}$ ,  $N_\omega = 100$ ,  $\omega_{p,t}^0 = 10^{-4} - p_{t-1}\sigma_p$ , and  $\Delta\omega = (10\sigma_p\sqrt{p_{t-1}} - \omega_{p,t}^0)/(N_\omega - 1)$ , as is performed by Bekaert et al. (2015) and South et al. (2019). Results are provided in Tables 7 and 8.

For the sequential version, we observe an improvement of up to  $2\times$  for 256-bit vector operations and almost  $3\times$  with 512-bit vector operations. This was not observed in the weak informativity test (Section 4), where there was diminishing returns from 512-bit vector operations. In the case of the BEGE inference, the BEGE cumulative distribution function approximation is a sufficiently large proportion of the total computation cost, and the efficient vectorisation of the calculation can exploit the longer 512-bit vectors.

As expected, we also see a compounding effect of vectorisation on the parallel versions of the SMC algorithm. However, the overall speedup factor varies. The significant difference in the parallelisation applied here and in previous sections, is that the SMC sampler requires threads to synchronise at the end of each iteration. This synchronisation in the resampling and annealing steps, and in estimating the optimal MCMC proposal scales, could be causing bottlenecks. This can be seen in the diminishing returns on the parallel speedups as the number of particles increases.

Table 7: Computational performance of the SMC sampler for BEGE parameter inference using an Intel Xeon E5-2680v3 (Haswell) processor. Parallel times are based on 4-way multithreading and SIMD times using 256-bit vector operations.

Configuration $N_p$	Runtime (Seconds) [Speedup factor]			
	sequential	sequential+SIMD	parallel	parallel+SIMD
250	5,224 [1.0×]	3,012 [1.7×]	3,314 [1.6×]	591 [8.8×]
500	10,372 [1.0×]	5,138 [2.0×]	3,125 [3.3×]	2,173 [4.8×]
750	18,781 [1.0×]	10,956 [1.7×]	5,696 [3.3×]	2,737 [6.7×]
1000	37,526 [1.0×]	19,989 [1.9×]	11,041 [3.4×]	7,415 [5.1×]

Table 8: Computational performance of the SMC sampler for BEGE parameter inference using an Intel Xeon Gold 6140 (Skylake) processor. Parallel times are based on 4-way multithreading and SIMD times using 512-bit vector operations.

Configuration $N_p$	Runtime (Seconds) [Speedup factor]			
	sequential	sequential+SIMD	parallel	parallel+SIMD
250	3,349 [1.0×]	1,144 [2.9×]	686 [4.8×]	256 [13.1×]
500	7,600 [1.0×]	2,651 [2.8×]	2,171 [3.5×]	669 [11.4×]
750	13,338 [1.0×]	4,718 [2.8×]	3,235 [4.1×]	1,985 [6.7×]
1000	20,338 [1.0×]	8,214 [2.5×]	8,006 [2.5×]	4,243 [4.7×]

## 5.4 Summary

In this last example, we demonstrate how vector operations can be used to further accelerate a parallel SMC sampler for a challenging inference problem from econometrics. It is important to note, however, that the log-likelihood approximation we apply, based on the work of Bekaert et al. (2015) is biased. Recently, Li et al. (2019) proposed an unbiased likelihood estimator, for which there are vectorisation opportunities also. However, for the purposes of this manuscript, we find the biased approximation of Bekaert et al. (2015) lends itself more direct discourse. Future work could focus on vectorised implementations of the unbiased estimator of Li et al. (2019).

## 6 Discussion

Across each of our example applications there have been some common features, which allow several conclusions to be drawn regarding task suitability for vectorisation. Firstly, it is clear that the form of stochastic model under study can have a dramatic effect on the potential performance boost due to vectorisation. This was particularly highlighted in the difference between continuous time and discrete time Markov processes, and may motivate the practitioner to consider alternative forms of related algorithms that are more suited to being vectorised. For example, by implementing approximations to the Gillespie algorithm rather than using its exact form (Section 3). Similarly, the success of the vectorised MCMC

proposal kernel for the analysis of weakly informative priors (Section 4) and the BEGE inference problem (Section 5) relied on the likelihood function being vectorised. Secondly, each application involved nested parallelisation. The utility of vectorisation here is that within each parallel thread, the computational tasks may be further sub-divided through use of SIMD operations. That is, efficiency gains due to vectorisation come in addition to those arising from the use of more general thread parallelisation. Finally, each application involved a mixture of tasks that can be performed completely independently and tasks that require synchronisation or communication. This is important, since independent parallel computation is ideal for multithreading and fine grain parallel operations with frequent synchronisation are well suited for vectorisation. These three features are common to many Bayesian applications, and as such, our demonstrations of SIMD operations combined with multithreading are widely applicable.

Many other Monte Carlo schemes can benefit from our approach, in fact, any application that has been demonstrated using a GPGPU could also exploit SIMD on the CPU (Lee et al., 2010). This is rarely taken into consideration when comparison between GPGPUs and CPUs are made, and is a source of misleading performance statistics which consequently favour GPGPU performance too highly (Hurn et al., 2016; Lee et al., 2010).

In the supporting information we have provided example C programs, using OpenMP and Intel’s MKL for parallel RNGs. However, we appreciate that, for very good reasons, higher level languages such as MATLAB and R are often the preferred environments for many practitioners. Certainly, the implementation techniques we present can be exploited through MATLAB C MEX or Rcpp interfaces, however, MATLAB and R must be configured correctly to use the required compiler options.

Unfortunately, many of the vectorisation and memory optimisations we presented cannot be directly exploited using a high level language alone. The only reliable way to access SIMD level parallelism from within a high level language is to use built-in matrix or vector functions that are already optimised (for example, by compiling R to use MKL). Here, a significant challenge is memory access. Between successive high level functions, it is unlikely that the caches are preserved, and as a result, our high performing Euler-Maruyama scheme and MCMC proposal cannot be directly replicated in MATLAB or R alone.

We have also presented realistic demonstrations in which Amdahl’s law truly affects the maximum performance gains that are possible through vectorisation. This is not a limitation of SIMD, but is rather the nature of parallel algorithms. In fact, the algorithm types that suit vector processing cannot always be efficiently implemented with threads.

There are many other Monte Carlo and Bayesian applications that could benefit from these approaches. One possibility is large scale SMC or particle filters, for example, the BEGE model with  $N_p > 10,000$ , perhaps operating within a pseudo-marginal scheme (Andrieu et al., 2010) with an unbiased likelihood estimator (Li et al., 2019). As demonstrated in Section 5, this can be implemented as a hybrid algorithm in which proposals and weight updates are performed in vectorised blocks that are distributed across multiple threads. However, on a large scale, such a scheme would need to reduce the synchronisation bottlenecks in resampling and annealing steps. A possible solution could involve the resam-

pling scheme of Murray et al. (2016) along with prefix summations for median expected squared jump distance calculations, that is, parallel computation of cumulative sums, to be performed (Hillis and Steele, 1986) in the resampling step, which may improve the performance. Another possibility is within the class of ABC validation or post-processing procedures. For example, in the recalibration post-processing technique of Rodrigues et al. (2018), each of the  $N$  samples  $\theta^*$  from the approximate posterior distribution are individually recalibrated by the construction of a further approximate (ABC) posterior for each  $\theta^*$  using all previously generated  $(\theta^*, \mathcal{D}^*)$  pairs, but based on observing the associated (simulated) dataset  $\mathcal{D}^*$ , and constructing all univariate marginal posterior cumulative distribution functions. This re-use of ABC algorithm and previously generated parameter values and datasets is very common in ABC (e.g. Blum et al., 2013), and makes them particularly suited for performance gains through parallelism and vectorisation.

Finally, in this article we have demonstrated that by following a few simple guidelines to maximise the utilisation of modern CPUs, advanced Monte Carlo methods may be relatively straightforwardly accelerated by a factor up to  $6\times$  in addition to further speedups obtained through multithreading. These techniques will only become more relevant in the future as CPUs architectures are released with wider vector processor units and statisticians develop more complex and sophisticated inferential algorithms.

**Acknowledgements** CD was supported by an Australian Research Council (ARC) Discovery Early Career Researcher Award (DE160100741). SAS was supported by the ARC under the Discovery Project scheme (DP160102544), and SAS and DJW by the Australian Centre of Excellence for Mathematical and Statistical Frontiers (ACEMS; CE140100049). Computational resources were provided by the eResearch Office, QUT. CD is grateful to ACEMS for providing funding to visit SAS at UNSW where discussions on this research took place. The authors thank Leah South and Dan Li for supplying useful MATLAB code for the BEGE example.

## References

- Amdahl, G. M. (1967). Validity of the single processor approach to achieving large scale computing capabilities. In *Proceedings of the April 18-20, 1967, Spring Joint Computer Conference*, AFIPS '67 (Spring), New York, NY, USA, pp. 483–485. ACM.
- Andrieu, C., A. Doucet, and R. Holenstein (2010). Particle Markov chain Monte Carlo methods. *Journal of the Royal Statistical Society: Series B* 72, 269–342.
- Barber, S., J. Voss, and M. Webster (2015). The rate of convergence for approximate Bayesian computation. *Electronic Journal of Statistics* 9, 80–195.
- Beaumont, M. A., W. Zhang, and D. J. Balding (2002). Approximate Bayesian computation in population genetics. *Genetics* 162, 2025–2035.

- Bekaert, G., E. Engstrom, and A. Ermolov (2015). Bad environments, good environments: A non-Gaussian asymmetric volatility model. *Journal of Economics* 186, 258–275.
- Beskos, A., A. Jasra, N. Kantas, and A. Thiery (2016). On the convergence of adaptive sequential Monte Carlo methods. *Annals of Applied Probability* 26, 1111–1146.
- Beskos, A., A. Jasra, K. Law, R. Tempone, and Y. Zhou (2017). Multilevel sequential Monte Carlo samplers. *Stochastic Processes and their Applications* 127, 1417–1440.
- Blum, M. G. B., M. A. Nunes, D. Prangle, and S. A. Sisson (2013). A comparative review of dimension reduction methods in approximate Bayesian computation. *Statistical Science* 28, 189–208.
- Bollerslev, T. (1986). Generalized autoregressive conditional heteroskedasticity. *Journal of Econometrics* 31(3), 307 – 327.
- Bonassi, F., L. You, and M. West (2011). Bayesian learning from marginal data in bionetwork models. *Statistical Applications in Genetics and Molecular Biology* 10(1), 49.
- Bradley, T., J. du Toit, R. Tong, M. Giles, and P. Woodhams (2011). Parallelization techniques for random number generators. In T. Green and R. Day (Eds.), *GPU Computing Gems Emerald Edition*. Elsevier Inc.
- Browning, A. P., S. W. McCue, R. N. Binny, M. J. Plank, E. T. Shah, and M. J. Simpson (2018). Inferring parameters for a lattice-free model of cell migration and proliferation using experimental data. *Journal of Theoretical Biology* 437, 251 – 260.
- Chopin, N. (2002). A sequential particle filter method for static models. *Biometrika* 89, 539–551.
- Crago, N. C., M. Stephenson, and S. W. Keckler (2018). Exposing memory access patterns to improve instruction and memory efficiency in GPUs. *ACM Transactions on Architecture and Code Optimization* 15(4), 45:1–45:23.
- Davies, R. and R. J. Brooks (2007). Stream correlations in multiple recursive and congruential generators. *Journal of Simulation* 1, 131–135.
- Del Moral, P., A. Doucet, and A. Jasra (2006). Sequential Monte Carlo samplers. *Journal of the Royal Statistical Society: Series B* 68, 411–436.
- Dodwell, T. J., C. Ketelsen, R. Scheichl, and A.-L. Teckentrup (2015). A hierarchical multi-level Markov chain Monte Carlo algorithm with applications to uncertainty quantification in subsurface flow. *SIAM/ASA Journal on Uncertainty Quantification* 3, 1075–1108.
- Dongarra, J., M. Gates, A. Haidar, Y. Jia, K. Kabir, P. Luszczek, and S. Tomov (2014). HPC programming on Intel many-integrated-core hardware with MAGMA port to Xeon Phi. *Scientific Programming* 2015.

- Drovandi, C. C. and A. N. Pettitt (2011). Estimation of parameters for macroparasite population evolution using approximate Bayesian computation. *Biometrics* 67(1), 225–233.
- Eddelbuettel, D. and R. Francois (2011). Rcpp: Seamless r and c++ integration. *Journal of Statistical Software, Articles* 40(8), 1–18.
- Edwards, H. C., C. R. Trott, and D. Sunderland (2014). Kokkos: Enabling manycore performance portability through polymorphic memory access patterns. *Journal of Parallel and Distributed Computing* 74(12), 3202 – 3216.
- Eichenberger, A. E., P. Wu, and K. O’Brien (2004). Vectorization for SIMD architectures with alignment constraints. *ACM SIGPLAN Notices* 39(6), 82–93.
- Engle, R. F. (1982). Autoregressive conditional heteroscedasticity with estimates of the variance of united kingdom inflation. *Econometrica* 50(4), 987–1007.
- Evans, M. and G. H. Jang (2011). Weak informativity and the information in one prior relative to another. *Statistical Science* 26, 423–439.
- Fan, Y. and S. A. Sisson (2018). ABC samplers. In S. A. Sisson, Y. Fan, and M. A. Beaumont (Eds.), *Handbook of Approximate Bayesian Computation*, pp. 87–123.
- Fearnhead, P. and D. Prangle (2012). Constructing summary statistics for approximate Bayesian computation: semi-automatic approximate Bayesian computation. *Journal of the Royal Statistical Society Series B* 74, 419–474.
- Fernandes, H., M. A. Aslam, J. Lobo, J. F. Ferreira, and J. Dias (2016). Bayesian inference implemented on FPGA with stochastic bitstreams for an autonomous robot. In *2016 26th International Conference on Field Programmable Logic and Applications (FPL)*, pp. 1–4.
- Gelman, A. (2006). Prior distributions for variance parameters in hierarchical models (Comment on an article by Browne and Draper). *Bayesian Analysis* 1, 515–534.
- Geng, T., E. Diken, T. Wang, L. Jozwiak, and M. Herbordt (2018). An access-pattern-aware on-chip vector memory system with automatic loading for SIMD architectures. In *2018 IEEE High Performance extreme Computing Conference (HPEC)*, pp. 1–7.
- Gillespie, D. T. (1977). Exact stochastic simulation of coupled chemical reactions. *The Journal of Physical Chemistry* 81, 2340–2361.
- Gillespie, D. T. (2000). The chemical Langevin equation. *The Journal of Chemical Physics* 113, 297–306.
- Gillespie, D. T. (2001). Approximate accelerated simulation of chemically reacting systems. *The Journal of Chemical Physics* 115, 1716–1733.

- Glosten, L. R., R. Jagannathan, and D. E. Runkle (1993). On the relation between the expected value and the volatility of the nominal excess return on stocks. *The Journal of Finance* 48(5), 1779–1801.
- Green, P. J., K. Łatuszyński, M. Pereyra, and C. P. Robert (2015). Bayesian computation: a summary of the current state, and samples backwards and forwards. *Statistics and Computing* 25, 835–862.
- Halyo, V., P. LeGresley, P. Lujan, V. Karpusenکو, and A. Vladimirov (2014). First evaluation of the CPU, GPGPU and MIC architectures for real time particle tracking based on Hough transform at the LHC. *Journal of Instrumentation* 9.
- Hillis, W. D. and G. L. Steele, Jr. (1986). Data parallel algorithms. *Communications of the ACM* 29, 1170–1183.
- Hurn, A. S., K. A. Lindsay, and D. J. Warne (2016). A heterogeneous computing approach to maximum likelihood parameter estimation for the heston model of stochastic volatility. In M. Nelson, D. Mallet, B. Pincombe, and J. Bunder (Eds.), *Proceedings of the 12th Biennial Engineering Mathematics and Applications Conference, EMAC-2015*, Volume 57 of *ANZIAM J.*, pp. C364–C381.
- Jasra, A., S. Jo, D. Nott, C. Shoemaker, and R. Tempone (2019). Multilevel Monte Carlo in approximate Bayesian computation. *Stochastic Analysis and Applications* 37(3), 346–360.
- Johnston, S. T., M. J. Simpson, D. L. S. McElwain, B. J. Binder, and J. V. Ross (2014). Interpreting scratch assays using pair density dynamics and approximate Bayesian computation. *Open Biology* 4(9), 140097.
- Klingbeil, G., R. Erban, M. Giles, and P. K. Maini (2011). STOCHSIMGPU: parallel stochastic simulation for the Systems Biology Toolbox 2 for MATLAB. *Bioinformatics* 27, 1170–1171.
- Kozlov, A. M., C. Goll, and A. Stamatakis (2014). Efficient computation of the phylogenetic likelihood function on the Intel MIC architecture. In *IEEE 28th International Parallel & Distributed Processing Symposium Workshops*.
- Lee, A., C. Yau, M. B. Giles, A. Doucet, and C. C. Holmes (2010). On the utility of graphics cards to perform massively parallel simulation of advanced Monte Carlo methods. *Journal of Computational and Graphical Statistics* 19, 769–789.
- Lee, V. W., C. Kim, J. Chhugani, M. Deisher, D. Kim, A. D. Nguyen, N. Satish, M. Smelyanskiy, S. Chennupaty, P. Hammarlund, R. Singhal, and P. Dubey (2010). Debunking the 100X GPU vs. CPU myth: An evaluation of throughput computing on CPU and GPU. *SIGARCH Computer Architecture News* 38, 451–460.
- Levesque, J. and G. Wagenbreth (2010). *High Performance Computing*. New York: Chapman and Hall/CRC.

- Li, D., A. Clements, and C. Drovandi (2019). Efficient Bayesian estimation for GARCH-type models via sequential Monte Carlo. *ArXiv e-prints*. arXiv:1906.03828v1 [stat.AP].
- Mahani, A. S. and M. T. A. Sharabiani (2015). SIMD parallel MCMC sampling with applications for big-data Bayesian analytics. *Computational Statistics and Data Analysis* 88, 75–99.
- Marjoram, P., J. Molitor, V. Plagnol, and S. Tavaré (2003). Markov chain Monte Carlo without likelihoods. *Proceedings of the National Academy of Sciences of the United States of America* 100, 15324–15328.
- Matsumoto, M. and T. Nishimura (1998, January). Mersenne twister: A 623-dimensionally equidistributed uniform pseudo-random number generator. *ACM Trans. Model. Comput. Simul.* 8(1), 3–30.
- Mikhailov, G. (2001). Some parallel Monte Carlo algorithms. In V. Malyshekin (Ed.), *Parallel Computing Technologies. PaCT 2001.*, Volume 2127 of *Lecture Notes in Computer Science*. Springer, Berlin, Heidelberg.
- Mudalige, G. R., I. Z. Reguly, and M. B. Giles (2016). Auto-vectorizing a large-scale production unstructured-mesh CFD application. In *Proceedings of the 3rd Workshop on Programming Models for SIMD/Vector Processing, WPMVP '16*, New York, NY, USA, pp. 5:1–5:8. ACM.
- Murray, L. M., A. Lee, and P. E. Jacob (2016). Parallel resampling in the particle filter. *Journal of Computational and Graphical Statistics* 25, 789–805.
- Nott, D., C. C. Drovandi, K. Mengersen, and M. Evans (2018). Approximate Bayesian computation predictive  $p$ -values with regression ABC. *Bayesian Analysis* 13, 59–83.
- Pasarica, C. and A. Gelman (2010). Adaptively scaling the metropolis algorithm using expected squared jumped distance. *Statistica Sinica* 20(1), 343–364.
- Pennycook, S. J., C. J. Hughes, M. Smelyanskiy, and S. A. Jarvis (2013). Exploring SIMD for molecular dynamics, using Intel® Xeon® processors and Intel® Xeon Phi coprocessors. In *2013 IEEE 27th International Symposium on Parallel and Distributed Processing*, pp. 1085–1097.
- Prangle, D. (2016). Lazy ABC. *Statistics and Computing* 26(1), 171–185.
- Press, W. H., S. A. Teukolsky, W. T. Vetterling, and B. P. Flannery (1992). *Numerical Recipes in C: The Art of Scientific Computing*. Cambridge University Press.
- Rodrigues, G. S., D. J. Nott, and S. A. Sisson (2019). Likelihood-free approximate Gibbs sampling. *arXiv:1906.04347*.
- Rodrigues, G. S., D. Prangle, and S. A. Sisson (2018). Recalibration: A post-processing method for approximate Bayesian computation. *Computational Statistics and Data Analysis* 126, 53–66.

- Ross, P. E. (2008). Why CPU frequency stalled. *IEEE Spectrum* 45, 72–72.
- Ross, R. J. H., R. E. Baker, A. Parker, M. J. Ford, R. L. Mort, and C. A. Yates (2017). Using approximate Bayesian computation to quantify cell–cell adhesion parameters in a cell migratory process. *npj Systems Biology and Applications* 3(1), 9.
- Salomone, R., L. F. South, C. C. Drovandi, and D. P. Kroese (2018). Unbiased and consistent nested sampling via sequential Monte Carlo. *ArXiv e-prints*. arXiv:1805.03924 [stat.CO].
- Sisson, S. A., Y. Fan, and M. Beaumont (2018). *Handbook of Approximate Bayesian Computation*. Chapman and Hall/CRC Press.
- Sisson, S. A., Y. Fan, and M. M. Tanaka (2007). Sequential Monte Carlo without likelihoods. *Proceedings of the National Academy of Sciences of the United States of America* 104, 1760–1765.
- South, L. F., A. N. Pettitt, and C. C. Drovandi (2019, 09). Sequential Monte Carlo samplers with independent Markov chain Monte Carlo proposals. *Bayesian Anal.* 14(3), 773–796.
- Sunnåker, M., A. G. Busetto, E. Numminen, J. Corander, M. Foll, and C. Dessimoz (2013). Approximate Bayesian computation. *PLoS Computational Biology* 9(1), e1002803.
- Tanaka, M. M., A. R. Francis, F. Luciani, and S. A. Sisson (2006). Using approximate Bayesian computation to estimate tuberculosis transmission parameter from genotype data. *Genetics* 173, 1511–1520.
- Tavaré, S., D. J. Balding, R. C. Griffiths, and P. Donnelly (1997). Inferring coalescence times from dna sequence data. *Genetics* 145(2), 505–518.
- Teodoro, G., T. Kurc, J. Kong, L. Cooper, and J. Saltz (2014). Comparative performance analysis of Intel Xeon Phi, GPU, and CPU: A case study from microscopy image analysis. In *Parallel and Distributed Processing Symposium, 2014 IEEE 28th International*.
- Terenin, A., S. Dong, and D. Draper (2018). GPU-accelerated Gibbs sampling: a case study of the horseshoe probit model. *Statistics and Computing*.
- Tian, X., H. Saito, S. V. Preis, E. N. Garcia, S. S. Kozhukhov, M. Masten, A. G. Cherkasov, and N. Panchenko (2013). Practical SIMD vectorization techniques for Intel® Xeon Phi coprocessors. In *2013 IEEE International Symposium on Parallel Distributed Processing, Workshops and Phd Forum*, pp. 1149–1158.
- Trobec, R., B. Slivnik, P. Bulić, and B. Robič (2018). *Introduction to Parallel Computing: From Algorithms to Programming on State-of-the-Art Platforms*. Cham: Springer International Publishing.
- van der Pas, R., E. Stotzer, E. Stotzer, and C. Terboven (2017). *Using OpenMP – The Next Step: Affinity, Accelerators, Tasking, and SIMD*. MIT Press.

- Vo, B. N., C. C. Drovandi, and A. N. Pettitt (2019). Bayesian parametric bootstrap for models with intractable likelihoods. *Bayesian Analysis* 14, 211–234.
- Vo, B. N., C. C. Drovandi, A. N. Pettitt, and M. J. Simpson (2015). Quantifying uncertainty in parameter estimates for stochastic models of collective cell spreading using approximate Bayesian computation. *Mathematical Biosciences* 263, 133 – 142.
- Wang, Q., Z. Xing, J. Liu, X. Qiang, C. Gong, and J. Jiang (2014). Parallel 3D deterministic particle transport on Intel MIC architecture. In *High Performance Computing Simulation (HPCS), 2014 International Conference on*, pp. 186–192.
- Warne, D. J., R. E. Baker, and M. J. Simpson (2018). Multilevel rejection sampling for approximate Bayesian computation. *Computational Statistics and Data Analysis* 124, 71–86.
- Warne, D. J., R. E. Baker, and M. J. Simpson (2019). Simulation and inference algorithms for stochastic biochemical reaction networks: from basic concepts to state-of-the-art. *Journal of the Royal Society Interface* 16, 20180943.
- Warne, D. J., N. A. Kelson, and R. F. Hayward (2014). Comparison of high level FPGA hardware design for solving tri-diagonal linear systems. *Procedia Computer Science* 29(Supplement C), 95 – 101.
- Zierke, S. and J. D. Bakos (2010). FPGA acceleration of the phylogenetic likelihood function for Bayesian MCMC inference methods. *BMC Bioinformatics* 11, 184.
- Zohouri, H. R., N. Maruyama, A. Smith, M. Matsuda, and S. Matsuoka (2016). Evaluating and optimizing opencl kernels for high performance computing with FPGAs. In *SC '16: Proceedings of the International Conference for High Performance Computing, Networking, Storage and Analysis*, pp. 409–420.